The Journal of Immunology

IL-10 Deficiency Reveals a Role for TLR2-Dependent Bystander Activation of T Cells in Lyme Arthritis

Sarah K. Whiteside, Jeremy P. Snook, Ying Ma, F. Lynn Sonderegger, Colleen Fisher, Charisse Petersen, James F. Zachary, June L. Round, Matthew A. Williams and Janis J. Weis

J Immunol published online 12 January 2018
http://www.jimmunol.org/content/early/2018/01/12/jimmunol.1701248

Supplementary Material **http://www.jimmunol.org/content/suppl/2018/01/12/jimmunol.1701248.DCSupplemental**

The Journal of Immunology is published twice each month by The American Association of Immunologists, Inc., 1451 Rockville Pike, Suite 650, Rockville, MD 20852

Print ISSN: 0022-1767 Online ISSN: 1550-6606.

Published January 12, 2018, doi:10.4049/jimmunol.1701248

IL-10 Deficiency Reveals a Role for TLR2-Dependent Bystander Activation of T Cells in Lyme Arthritis

Sarah K. Whiteside,* Jeremy P. Snook,* Ying Ma,* F. Lynn Sonderegger,* Colleen Fisher,* Charisse Petersen,* James F. Zachary,† June L. Round,* Matthew A. Williams,* and Janis J. Weis*

T cells predominate the immune responses in the synovial fluid of patients with persistent Lyme arthritis; however, their role in Lyme disease remains poorly defined. Using a murine model of persistent Lyme arthritis, we observed that bystander activation of CD4$^+$ and CD8$^+$ T cells leads to arthritis-promoting IFN-γ, similar to the inflammatory environment seen in the synovial tissue of patients with posttreatment Lyme disease. TCR transgenic mice containing monoclonal specificity toward non–*Borrelia* epitopes confirmed that bystander T cell activation was responsible for disease development. The microbial pattern recognition receptor TLR2 was upregulated on T cells following infection, implicating it as marker of bystander T cell activation. In fact, T cell–intrinsic expression of TLR2 contributed to IFN-γ production and arthritis, providing a mechanism for microbial-induced bystander T cell activation during infection. The IL-10–deficient mouse reveals a novel TLR2-intrinsic role for T cells in Lyme arthritis, with potentially broad application to immune pathogenesis. ***The Journal of Immunology*****, 2018, 200: 000–000.**

Lyme disease, caused by the tick-borne spirochete *Borrelia burgdorferi*, is the most common vector-borne illness in North America with estimates of 300,000 cases annually (1). The most common late manifestation of Lyme disease is arthritis, with up to 60% of infected individuals reporting intermittent attacks of joint swelling and pain (2). This can usually be treated successfully with 1–2 mo of oral or i.v. antibiotics (1, 3). However, 10–20% of patients present with persistent arthritis for months or years after standard antibiotic regimen, referred to as antibiotic-refractory arthritis or posttreatment Lyme disease (4, 5). Patients are negative for the presence of *B. burgdorferi* DNA after standard antibiotic therapy, raising several questions regarding the etiology of this long-lasting illness (6–8). Persistent Lyme arthritis shares certain pathogenic themes with rheumatoid arthritis such as similar synovial lesions, a dominant Th1 CD4$^+$ T cell response in synovial tissues, and high concentrations of proinflammatory chemoattractants for CD4$^+$ and CD8$^+$ T cells in synovial fluid (9–11).

Several hypotheses have been proposed to explain persistent symptoms following antibiotic treatment, including molecular mimicry, dysregulated inflammation, and persistence of bacterial Ags (12–18). Adoptive transfer of CD4$^+$ T cells into Rag1-deficient mice, which lack B and T cells, exacerbated the severity of arthritis and suggested a role for dysregulated T cells in Lyme disease (19). More than 8% of the *B. burgdorferi* genome coding sequences are specific for Pam3Cys-modified lipoproteins, which possess the potent ability to stimulate host immune responses by interacting with TLR1/2 heterodimers (20–24). Experiments with TLR2 whole-body knockout mice have demonstrated a compromised host defense and T cell involvement (25–27). Additionally, TLR2 expression on T cells has been shown to act as a costimulatory signal for T cell activation (28–30), and it could potentially be playing a role in inappropriate T cell responses during *B. burgdorferi* infection.

There have been numerous reports implicating a variety of CD4$^+$ T cells in the pathogenesis of human Lyme disease (9, 31–37). Studies have characterized patients with persistent symptoms as having Th1 CD4$^+$ T cells and inflammatory cytokines and chemokines such as IFN-γ, IL-1β, IL-6, CXCL9, and CXCL10 present in the synovial fluid, sometimes even months following infection and treatment (31, 32). IL-10$^{-/-}$ mice, which lack the anti-inflammatory mediator IL-10, exhibit transcriptional upregulation of these same inflammatory mediators found in patients, contain CD4$^+$ T cells in the joints, and have elevated IFN-γ in the serum at 2 wk postinfection despite extremely low levels of *B. burgdorferi* in the joint tissue (38, 39). The absence of IL-10 exposes the pathogenic potential of T cells whose activation threshold has been lowered during *B. burgdorferi* infection. We have used the IL-10$^{-/-}$ mouse as a model for persistent Lyme arthritis to further investigate the arthritis-promoting properties of CD4$^+$ T cells and IFN-γ in response to *B. burgdorferi* infection.

*Department of Pathology, University of Utah, Salt Lake City, UT 84112; and †Department of Pathobiology, University of Illinois at Urbana–Champaign, Urbana, IL 61802

ORCIDs: 0000-0003-4354-4713 (S.K.W.); 0000-0002-1396-9254 (J.P.S.); 0000-0002-3688-6283 (C.F.); 0000-0003-4045-2610 (C.P.); 0000-0001-7214-5987 (J.J.W.).

Received for publication August 29, 2017. Accepted for publication December 13, 2017.

S.K.W. was supported by National Institutes of Allergy and Infectious Disease Research Training Grant T32 AI055434. J.P.S. was supported by the American Association of Immunologists Careers in Immunology Fellowship Program. J.L.R. was supported by the Edward Mallinckrodt Jr. Foundation, the Pew Charitable Trusts Scholars Program, National Science Foundation CAREER Award IOS-1253278, a David and Lucile Packard Foundation Fellowship in Science and Engineering, National Institute of Allergy and Infectious Diseases Grants K22 AI95375, AI107090, and AI109122, and by National Institutes of Health Directors Innovator Award DP2AT008746. J.J.W. and M.A.W. were supported by National Institutes of Health Grant R01 AI32223. J.J.W. was supported by National Institutes of Health Grants R01 AR43521 and R21AI114462. Flow cytometry cell sorting was supported by National Center for Research Resources/National Institutes of Health Grant 1S10RR026802-01.

Address correspondence and reprint requests to Dr. Janis J. Weis, Department of Pathology, Division of Microbiology and Immunology, University of Utah Health Science Center, 15 North Medical Drive East, Salt Lake City, UT 84112. E-mail address: Janis.weis@path.utah.edu

The online version of this article contains supplemental material.

Abbreviations used in this article: LCMV, lymphocytic choriomeningitis virus; qRT-PCR, quantitative RT-PCR; Vβ, β-chain V region; WT, wild-type.

Despite correlative evidence linking aberrant T cell responses to other inflammatory arthritis diseases such as rheumatoid arthritis (40), the role of dysregulated T cell responses in the development of persistent Lyme arthritis has yet to be elucidated. In the current study, we show that activation of either $CD4^+$ or $CD8^+$ T cells is required for the development of Lyme arthritis, which persists in the presence of extremely low levels of *B. burgdorferi* Ag. Using transgenic mouse models, we demonstrate that T cell activation occurs independent of *Borrelia*-specific TCR interaction. Furthermore, we show that *B. burgdorferi* infection increases TLR2 expression on T cells. Cell transfer experiments revealed TLR2 as a critical mediator of T cell activation following *B. burgdorferi* infection, which results in enhanced IFN-γ production and Lyme arthritis. These results identify a novel mechanism of Lyme arthritis development dependent on TLR2 bystander activation of $CD4^+$ and $CD8^+$ T cells.

Materials and Methods

Experimental animals

C57BL/6, C57BL/6 IL-$10^{-/-}$ (B6.129P2-*Il10*^{tm1Cgn}/J), C57BL/6 TCRα$^{-/-}$ (B6.129S2-*Tcra*^{tm1Mom}/J), C57BL/6 Rag1$^{-/-}$ (B6.129S7-*Rag1*^{tm1Mom}/J), and C57BL/6 TLR2$^{-/-}$ (B6.129-*Tlr2*^{tm1Kir}/J) mice were obtained from The Jackson Laboratory. C57BL/6 Rag2$^{-/-}$/OT-I mice were purchased from Taconic. SMARTA TCR transgenic mice, specific for the immunodominant class II–restricted epitope of lymphocytic choriomeningitis virus (LCMV) $gp_{61–80}$ (41), were maintained on a C57BL/6 background and additionally crossed to IL-$10^{-/-}$ mice (SMARTA/IL-$10^{-/-}$ mice). SMARTA/IL-$10^{-/-}$ mice were further crossed to TCRα$^{-/-}$ mice. Rag2$^{-/-}$/OT-I mice were crossed to IL-$10^{-/-}$ mice. Genotyping was performed according to protocol provided by The Jackson Laboratory for the IL-10 and TCRα mutation. Experiments were performed using mice 5–7 wk of age, with male and female mice equally distributed into experiment and control groups. To prevent colitis development, IL-$10^{-/-}$, SMARTA/TCRα$^{-/-}$/IL-$10^{-/-}$, and OT-I/Rag2$^{-/-}$/IL-$10^{-/-}$ mice were kept on antibiotic water (trimethoprim and sulfamethoxazole) until 1 d prior to infection. Mouse colonies were housed in the pathogen-free facility at the University of Utah. All mice used in this study were cared for in accordance with the guidelines of the Institutional Animal Care and Use Committee of the National Institutes of Health, and all animal experiments were approved by the Institutional Animal Care and Use Committee.

Bacteria strain and infection of mice

The N40 isolate of *B. burgdorferi* (provided by S. Barthold, University of California, Davis, CA) was grown to late log phase in Barbour–Stoenner–Kelly-II medium supplemented with 6% rabbit serum (Sigma-Aldrich). Mice were infected with 2×10^4 *B. burgdorferi* by intradermal injection into the skin of the back. Infection was confirmed in mice sacrificed at 1 and 2 wk by the culture of *B. burgdorferi* from the bladder as described (25). ELISA quantification of *B. burgdorferi*–specific IgM and IgG concentrations was used to confirm infection in mice sacrificed at and after 14 d of infection as previously published (25). To measure in vivo cytokine production, mice were injected i.v. with 0.25 mg of brefeldin A (Sigma-Aldrich) in PBS 6 h before sacrifice (42).

Assessment of arthritis severity

Ankle measurements were obtained using a metric caliper before and 4 wk after infection by an investigator blinded to the experimental group. Rear ankle joints were prepared for assessment of histopathologic lesions by removal of the skin, and tissue was fixed in 10% neutral buffered formalin. Joints were decalcified and embedded in paraffin, sectioned at 3 μm, and stained with H&E. Lesions were scored in a blinded fashion, with each slide receiving a score of 0–5 for the characteristics of the disease such as polymorphonuclear leukocyte and mononuclear cell (lymphocytes, monocytes, macrophages) infiltration into inflammatory processes, tendon sheath thickening (hypertrophy and hyperplasia of surface cells and/or underlying dense sheets of cells resembling immature fibroblasts, synoviocytes, and/or granulation tissue), reactive/reparative responses (periosteal hyperplasia and new bone formation and remodeling), and overall lesion (composite score based on all lesions observed in six to eight sections per joint), with 5 representing the most severe lesion, and 0 representing no lesion as previously described (43).

Injection of mAbs

Abs used in neutralized or depletion studies were purchased from Bio X Cell and were aggregate and endotoxin free, and sterile. Cellular subsets were depleted by administering 0.2 mg of Ab into the i.p. cavity every 4 d beginning 1 d prior to infection as indicated: anti-CD4 (GK1.5) and anti-CD8 (YTS 169.4). Rat IgG2b (LTF-2) was used as the isotype control. IFN-γ was neutralized using 1 mg of anti–IFN-γ (XMG1.2) 1 d prior to infection, followed by additional doses of 0.5 mg of anti–IFN-γ every 4–5 d. Rat IgG1 (HRPN) was used as the isotype control for IFN-γ neutralization. Cellular depletions of $CD4^+$ and $CD8^+$ T cells were confirmed by flow cytometry (Supplemental Fig. 2).

Intracellular staining, restimulation, and isolation of T cells

$CD3^+CD4^+$ and $CD3^+CD8^+$ T cells were isolated from popliteal and inguinal lymph nodes for intracellular cytokine staining. For mice treated with brefeldin A, 1×10^6 cells were stained with surface markers and incubated for 30 min at 4°C. Cells were fixed/permeabilized in 100 μl of Cytofix/Cytoperm (BD Biosciences). Cells were resuspended in 100 μl of Perm/Wash buffer with fluorochrome-conjugated IFN-γ, briefly vortexed, and incubated on ice in the dark for 45 min. Cells were resuspended in 200 μl of PBS plus 2% FBS for analysis by flow cytometry. Restimulation of IL-$10^{-/-}$, SMARTA/TCRα$^{-/-}$/IL-$10^{-/-}$, and OT-I/Rag2$^{-/-}$/IL-$10^{-/-}$ cells was performed for 4 h with 20 ng/ml PMA and 1 μM ionomycin at 37°C in the presence of brefeldin A (1 μl/ml; GolgiPlug). For cell transfer experiments, $CD3^+CD4^+$ and $CD3^+CD8^+$ T cells were isolated from lymph nodes (popliteal and inguinal) and spleens of wild-type (WT) C57BL/6 and TLR2$^{-/-}$ mice using the Pan T Cell Isolation Kit II (Miltenyi Biotec). T cell sorting purity was determined by flow cytometry.

Phosphorylation of ZAP-70

Splenocytes from naive SMARTA/TCRα$^{-/-}$/IL-$10^{-/-}$ and OT-I/Rag2$^{-/-}$/IL-$10^{-/-}$ were isolated and 1×10^6 cells were stimulated for 3 h at 37°C in the presence of 1 μM $gp_{61–80}$ peptide (GLKGPDIYKGVYQFKSVEFD), 1 μM $OVA_{257–264}$ peptide (SIINFEKL), or 5 μg/ml sonicated *B. burgdorferi*. Unstimulated cells incubated with media alone were used as a control. After stimulation, cells were fixed in 100 μl of 1.5% paraformaldehyde and incubated at 37°C for 10 min. After fixation, cells were stained with surface markers CD4, CD8, and Vα2 in PBS containing 2% FBS for 25 min on ice in the dark. Cells were permeabilized using 100 μl of cold 100% methanol for 10 min on ice. Cells were centrifuged and resuspended in 100 μl of PBS containing 2% FBS with pZAP-70/SYK (Y319/Y352) clone n3kobu5 (eBioscience) and incubated on ice in the dark for 45 min. Total ZAP-70 clone 1E7.2 (eBioscience) was used as a control. ZAP-70 phosphorylation was analyzed using flow cytometry.

Isolation of RNA and quantitative RT-PCR

RNA was purified from the tibiotarsal joints after the skin had been removed. Tissue was immediately immersed in RNA stabilization solution (Invitrogen) and stored at −80°C. Total RNA was recovered from homogenized tissue using the Direct-zol kit (Zymo Research). RNA recovered from tissue and cells was reverse transcribed, and transcripts were quantified using a Roche LC-480 quantitative RT-PCR (qRT-PCR) machine according to our previously described protocols (44). Primer sequences used in this study were as follows: *CD8β* (CD8), forward, 5′-CTCTGGCTGGTCTTCAGTATGA-3′, reverse, 5′-TCTTTGCCGTATGGTTGGTTT-3′; *TLR2*, forward, 5′-TTGAAGAACTCAGCCTGTAAG-3′, reverse, 5′-GCTTCCAGAGTCTCCAGTTTG-3′. Primer sequences for *B. burgdorferi 16S rRNA* (45), *β-actin* (44), *CD4* (38), *Ifng* and *Cxcl9* (46), and *Cxcl10* (38) can be found in the indicated citations.

Flow cytometry

Flow cytometry data were collected on an LSRFortessa (BD Biosciences) flow cytometer and analyzed using FlowJo (v.10) software. FACS cell sorting was performed using FACSAria (BD Biosciences). Confirmation of cell sorting efficiency was performed using qRT-PCR. Cell surface stains were done in PBS containing 2% FBS. Intracellular stains for cytokines were done using a kit per the manufacturer's instructions (BD Biosciences). Position of gates for sorting and analysis was based on analysis of appropriate isotype controls. Fluorochrome-conjugated Abs from BioLegend were CD3ε, CD4, CD8α, CD19, CD44, CD62L, IFN-γ, NK1.1, and Vα2. Fluorochrome-conjugated Abs from eBioscience were TLR2 and pZAP-70.

ELISA analysis of mouse serum

Blood was obtained from the tail vein of mice 2 wk postinfection and collected by submandibular puncture at the time of sacrifice. Serum was

isolated and stored at −20°C prior to analysis. IFN-γ concentrations in serum samples were detected by sandwich ELISA using clone R4-6A2 as the capture Ab, and biotinylated Ab (XMG1.2) for detection. To determine *B. burgdorferi*–specific IgM and IgG concentrations, microtiter plates were coated with either sonicated *B. burgdorferi* or goat Ab to mouse IgG and IgM (Life Technologies). Serum dilutions were added to plates for 90 min at 37°C and bound murine Ig was detected by addition of HRP-conjugated Abs to murine IgG or IgM (Thermo Fisher Scientific). Ig content was estimated by comparing with standard curves using purified IgG or IgM as previously described (25).

Quantification and statistical analysis

The number of mice per group is annotated in corresponding figure legends. Statistical analysis was performed using Prism 6.0d software. Multiple-sample data sets were analyzed by one-way ANOVA followed by a Bonferroni post hoc test for pairwise comparisons, as appropriate and indicated in figure legends. Two-sample data sets were analyzed by a Student *t* test. Categorical data for histopathology were assessed by a Mann–Whitney *U* test. In all figures, data represent the mean ± SEM. A p value ≤ 0.05 was considered significant (*$p \leq 0.05$, **$p \leq 0.01$, ***$p \leq 0.001$, ****$p \leq 0.0001$).

Results

Lyme arthritis is persistent and sustained in the absence of IL-10

The involvement of CD4$^+$ T cells in the pathogenesis of human Lyme disease is seen even months following infection (9, 10), prompting investigation of a model that would allow assessment of the contribution of T cells. We have shown previously that the mild arthritis in C57BL/6 mice is increased in the absence of IL-10 despite greatly reduced numbers of *B. burgdorferi* in the joint tissue (38, 47). To determine whether C57BL/6 IL-10$^{-/-}$ mice could be used as a model of the persistent Lyme arthritis seen in human patients, infected mice were followed for 18 wk. *B. burgdorferi 16S rRNA* was no longer detectable in the joint tissue of IL-10$^{-/-}$ mice at this time (Table I). Additionally, IL-10$^{-/-}$ mice displayed sustained upregulation of *Ifng*, *Cxcl9*, and *Cxcl10* transcripts in the joint tissue (Table I), similar to observations in the synovial fluid of human patients months following antibiotic therapy (48, 49). In contrast, arthritis-resistant WT C57BL/6 mice continued to harbor detectable amounts of *B. burgdorferi* 18 wk postinfection; however, *Ifng*, *Cxcl9*, and *Cxcl10* transcripts were not upregulated in the joint tissue (Table I). These results suggest that IL-10$^{-/-}$ mice are a suitable model for the investigation of the arthritis-promoting properties of CD4$^+$ T cells and IFN-γ in *B. burgdorferi* infection, as seen in human patients. This has not been possible in the widely studied C3H mouse, where neither T cells nor IFN-γ is required for arthritis development (46, 50, 51).

CD4$^+$ and CD8$^+$ T cells from B. burgdorferi*–infected mice produce IFN-γ: ex vivo analysis*

Localized IFN-γ production has been observed in the synovial fluid of patients with persistent symptoms (52). Similarly, arthritis development in IL-10$^{-/-}$ mice is dependent on both systemic and localized production of IFN-γ (38). Canonical sources of IFN-γ include Th1 CD4$^+$ T cells, NK cells, and NKT cells, all of which are found in the joint tissue of *B. burgdorferi*–infected IL-10$^{-/-}$ mice (38, 53). To define the cellular sources of IFN-γ in Lyme arthritis development, IL-10$^{-/-}$ mice were infected with *B. burgdorferi* and cells were harvested from the draining popliteal and inguinal lymph nodes 4 wk postinfection, which is the peak of arthritis severity. Cells were restimulated in the presence of PMA and ionomycin for 4 h and then intracellularly stained for IFN-γ and analyzed by flow cytometry. This allowed for the identification of cells poised to produce IFN-γ. The frequency of both CD4$^+$IFN-γ$^+$ and CD8$^+$IFN-γ$^+$ T cells was increased compared with mock-infected mice (Fig. 1A). IFN-γ was not produced by NK or NKT cells in response to PMA/ionomycin stimulation (data not shown), thus suggesting that most IFN-γ–producing cells were T cells. The production of IFN-γ is specific to the draining lymph nodes, as T cells do not produce IFN-γ in other secondary lymphoid organs such as the spleen (data not shown). These proportional increases in IFN-γ$^+$ lymphocyte populations were also reflected in total cell numbers (Fig. 1B). Furthermore, CD4$^+$ and CD8$^+$ T cells were producing more IFN-γ on a per cell basis compared with controls (Fig. 1B). Interestingly, although there were fewer IFN-γ$^+$–producing CD4$^+$ T cells than CD8$^+$ T cells, CD4$^+$ T cells were secreting more IFN-γ than CD8$^+$ T cells as measured by mean fluorescence intensity. Taken together, these data suggest that both CD4$^+$ and CD8$^+$ T cells are poised to make IFN-γ following *B. burgdorferi* infection.

CD4$^+$ and CD8$^+$ T cells produce IFN-γ in vivo throughout B. burgdorferi *infection*

To capture the actual in vivo cytokine production during the course of *B. burgdorferi* infection, infected IL-10$^{-/-}$ mice were injected i.v. with the Golgi blocking agent, brefeldin A, 6 h prior to sacrifice (42). CD4$^+$ and CD8$^+$ T cells were analyzed for activation and functional markers by flow cytometry. Intracellular staining revealed an increase in the frequency and number of CD4$^+$ and CD8$^+$ T cells producing IFN-γ throughout infection (Fig. 1C, 1D). Importantly, the numbers of both CD4$^+$IFN-γ$^+$ and CD8$^+$IFN-γ$^+$ T cell were equivalent by 4 wk postinfection, demonstrating that both are playing a critical role in IFN-γ production (Fig. 1D). At 4 wk postinfection, during peak arthritis severity, both CD4$^+$ and CD8$^+$ T cells had expanded ∼3-fold, suggesting that both CD4$^+$ and CD8$^+$ T cells are either trafficking to or proliferating in the draining lymph nodes during arthritis development (Supplemental Fig. 1). CD44 expression was assessed as an additional indicator of T cell activation status. Both the frequency and total number of CD4$^+$CD44^{hi} and CD8$^+$CD44^{hi} T cells increased throughout infection, demonstrating that *B. burgdorferi* induces activation of both CD4$^+$ and CD8$^+$ T cells (Fig. 1E, 1F). Taken together, these data indicate that CD4$^+$ and CD8$^+$ T cells are expanding in the

Table I. Arthritis and inflammatory mediators are sustained for 18 wk in joint tissue of *B. burgdorferi*–infected IL-10$^{-/-}$ mice

Mouse Genotype	Infection	Arthritis (Δmm)	Transcript/1000 β-*actin*				
			Ifng	*Cxcl9*	*Cxcl10*	*Il10*	*B. burgdorferi 16S rRNA*
C57BL/6	Mock	0.01 ± 0.01	0.04 ± 0.02	3.70 ± 0.65	1.91 ± 058	ND	ND
	Bb	0.10 ± 0.04	0.05 ± 0.02	6.68 ± 1.21	1.94 ± 1.9	**0.08 ± 0.02**	**9.43 ± 4.90**
C57BL/6 IL-10$^{-/-}$	Mock	0.01 ± 0.01	0.06 ± 0.02	6.93 ± 1.53	1.80 ± 0.53	ND	ND
	Bb	**0.64 ± 0.5**	**2.12 ± 0.45**	**249 ± 45.18**	**21.14 ± 2.62**	ND	ND

C57BL/6 and IL-10$^{-/-}$ mice were infected with *B. burgdorferi* for 18 wk, after which joints were harvested for analysis of inflammation and bacterial burden. Transcripts for *Ifng*, *Cxcl9*, *Cxcl10*, *Il10*, and *B. burgdorferi*–specific *16S rRNA* were measured by qRT-PCR and normalized to β-*actin*. Values for infected mice that are significantly different from mock-infected are indicated in bold ± SEM ($n \geq 3$ per group), by a Student *t* test ($p < 0.01$). ND, not detected.

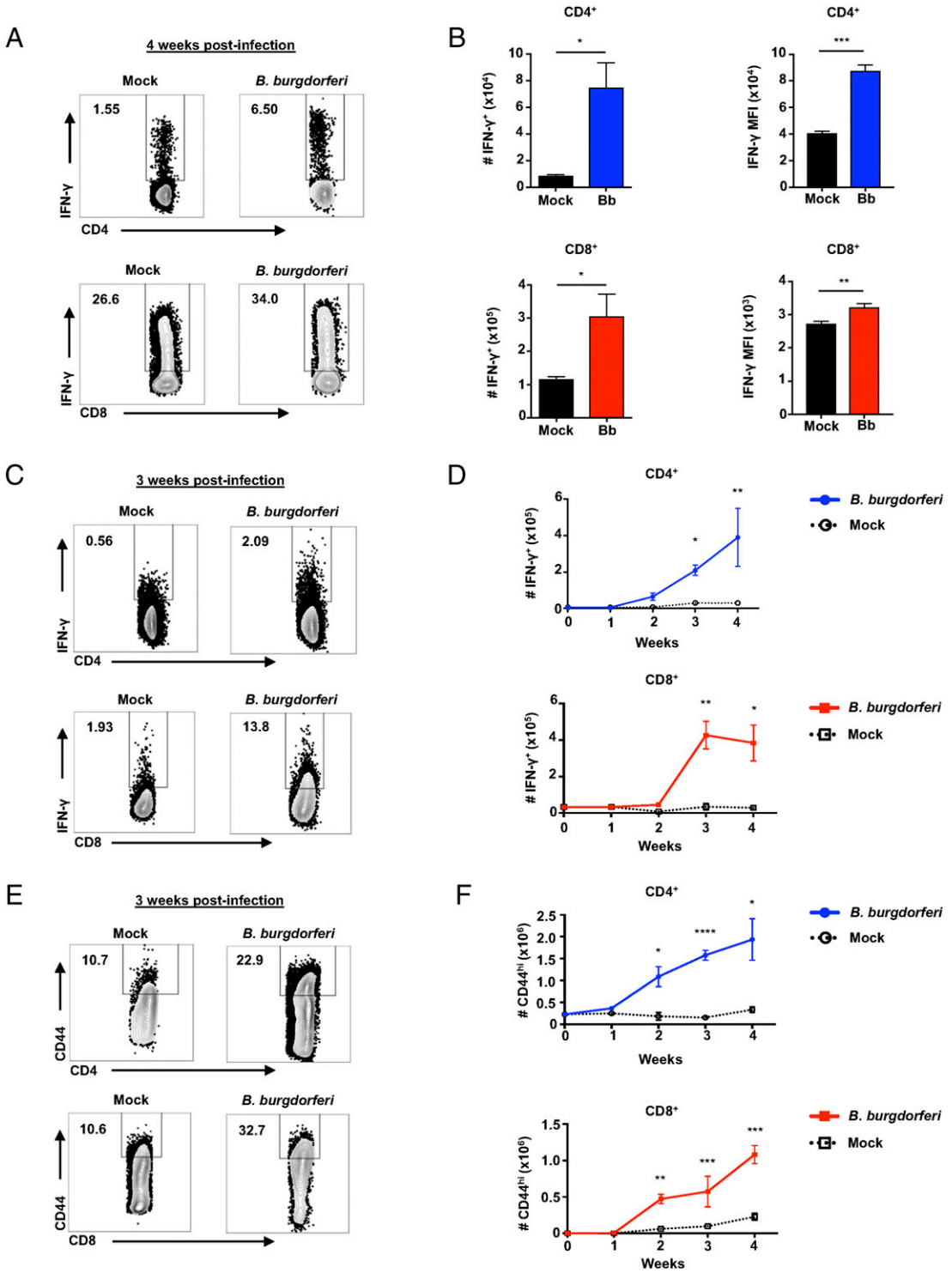

FIGURE 1. CD4$^+$ and CD8$^+$ T cells produce IFN-γ throughout *B. burgdorferi* infection. IL-10$^{-/-}$ mice were infected with *B. burgdorferi*, after which popliteal and inguinal lymph nodes were collected for analysis of T cells and IFN-γ production. (**A**) *B. burgdorferi*–infected or mock-infected IL-10$^{-/-}$ mice were sacrificed after 4 wk of infection. Representative flow plots of IFN-γ production by CD4$^+$ and CD8$^+$ T cells in after 4 h of stimulation with PMA/ionomycin in presence of brefeldin A. Numbers in upper left corner of boxes are percentage IFN-γ$^+$ cells. (**B**) Total number of IFN-γ$^+$CD4$^+$ and IFN-γ$^+$ CD8$^+$ T cells by flow cytometry and the mean fluorescence intensity (MFI) of IFN-γ. (**C**–**F**) *B. burgdorferi*–infected or mock-infected IL-10$^{-/-}$ mice were injected with brefeldin A 6 h before sacrifice at 1 wk time intervals for 4 wk. (C) Representative flow plots of IFN-γ production by CD4$^+$ and CD8$^+$ T cells in *B. burgdorferi*–infected or mock-infected IL-10$^{-/-}$ mice at 3 wk of infection. Numbers in upper left corner of boxes are percentage IFN-γ$^+$ cells. (D) Total number of CD4$^+$IFN-γ$^+$ and CD8$^+$IFN-γ$^+$ T cells from infected and mock-infected IL-10$^{-/-}$ mice. (E) Representative flow plots of CD4$^+$CD44^{hi} and CD8$^+$CD44^{hi} T cells in *B. burgdorferi*–infected or mock-infected IL-10$^{-/-}$ mice. Numbers in upper left corner of boxes are percentage CD44^{hi} cells. (F) Total number of CD4$^+$CD44^{hi} and CD8$^+$CD44^{hi} T cells from infected and mock-infected IL-10$^{-/-}$ mice. Error bars indicate the SEM ($n \geq 3$ per group). Data are representative of two independent experiments. *$p < 0.05$, **$p < 0.01$, ***$p < 0.001$, ****$p < 0.0001$, for differences between groups by Student *t* test.

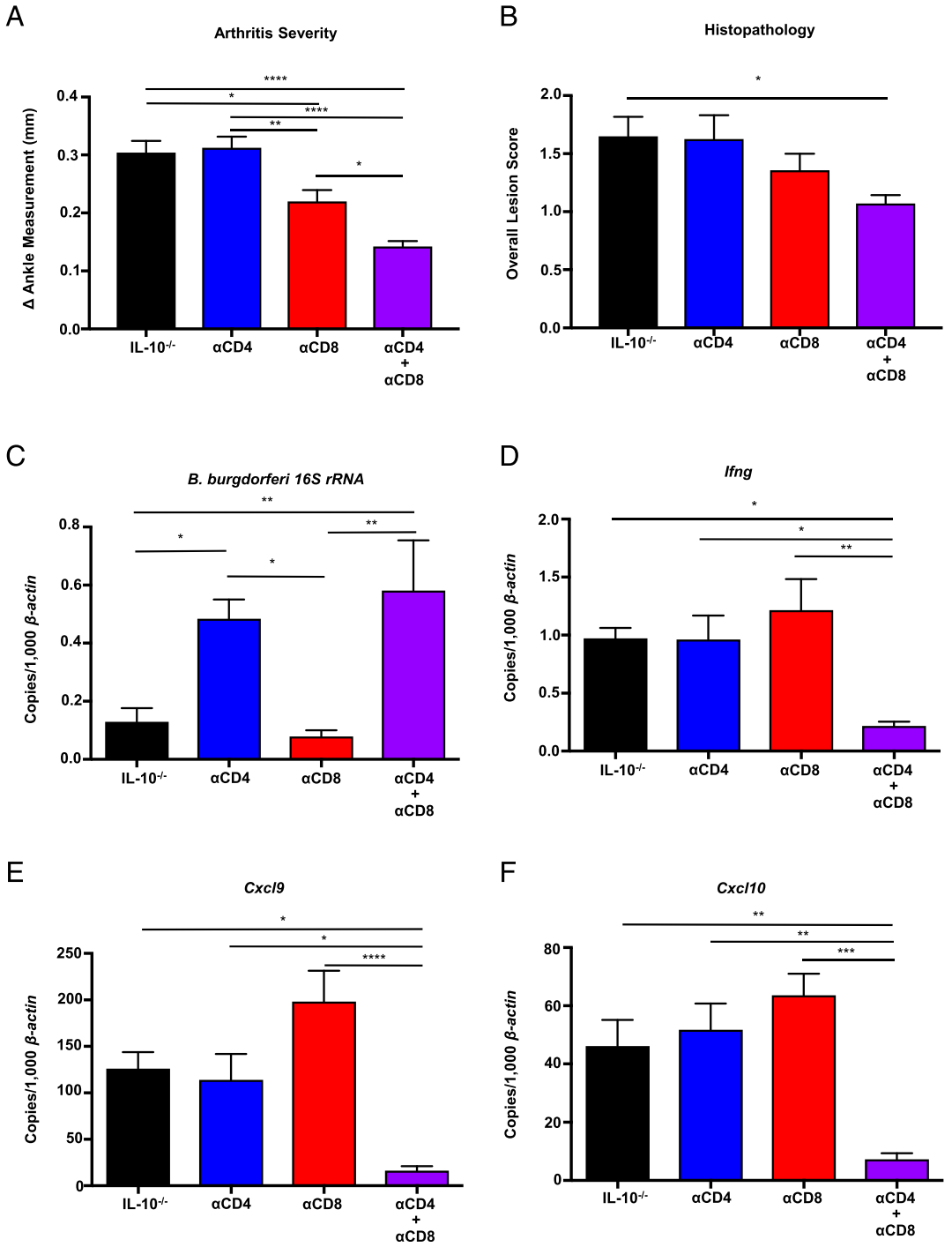

FIGURE 2. Both $CD4^+$ and $CD8^+$ T cells contribute to the development of Lyme arthritis. IL-$10^{-/-}$ mice were infected with *B. burgdorferi* for 4 wk and treated with isotype control Ab, anti-CD4, anti-CD8, or both anti-CD4 and anti-CD8 throughout the infection (see *Materials and Methods*). (**A**) Rear ankle measurements were taken before infection and 4 wk postinfection, and the change in ankle measurement is shown. (**B**) The most swollen ankle was assessed by histopathologic evaluation. Scores of 0–5, with 5 being most severe, were assigned to each sample. (**C**–**F**) Quantification of *B. burgdorferi*–specific *16S rRNA*, *Ifng*, *Cxcl9*, and *Cxcl10* was normalized to 1000 *β-actin* in the joint using qRT-PCR. Error bars indicate the SEM ($n \geq 7$ per group). $*p < 0.05$, $**p < 0.01$, $***p < 0.001$, $****p < 0.0001$, between groups by ANOVA followed by a Bonferroni post hoc test (A and C–F). (B) For lesion scoring, a Mann–Whitney *U* test was used to determine whether there was statistically significant difference with groups, with the *p* value indicated.

draining lymph nodes upon *B. burgdorferi* infection and they are functionally active as demonstrated through increased IFN-γ production and CD44 expression.

Both $CD4^+$ and $CD8^+$ T cells contribute to the development of Lyme arthritis

Because $CD4^+$ and $CD8^+$ T cells are the primary cellular sources of IFN-γ in the draining lymph nodes, we hypothesized that they were both necessary and sufficient for the development of Lyme arthritis in IL-$10^{-/-}$ mice following *B. burgdorferi* infection. To directly assess the contribution of $CD4^+$ and $CD8^+$ T cells, *B. burgdorferi*–infected IL-$10^{-/-}$ mice were treated with depleting Abs directed toward CD4, CD8, or a combination of both throughout infection (see *Materials and Methods*). Depletion efficiency was measured throughout the length of the experiment by flow cytometric analysis of blood, and also analyzed at the time of

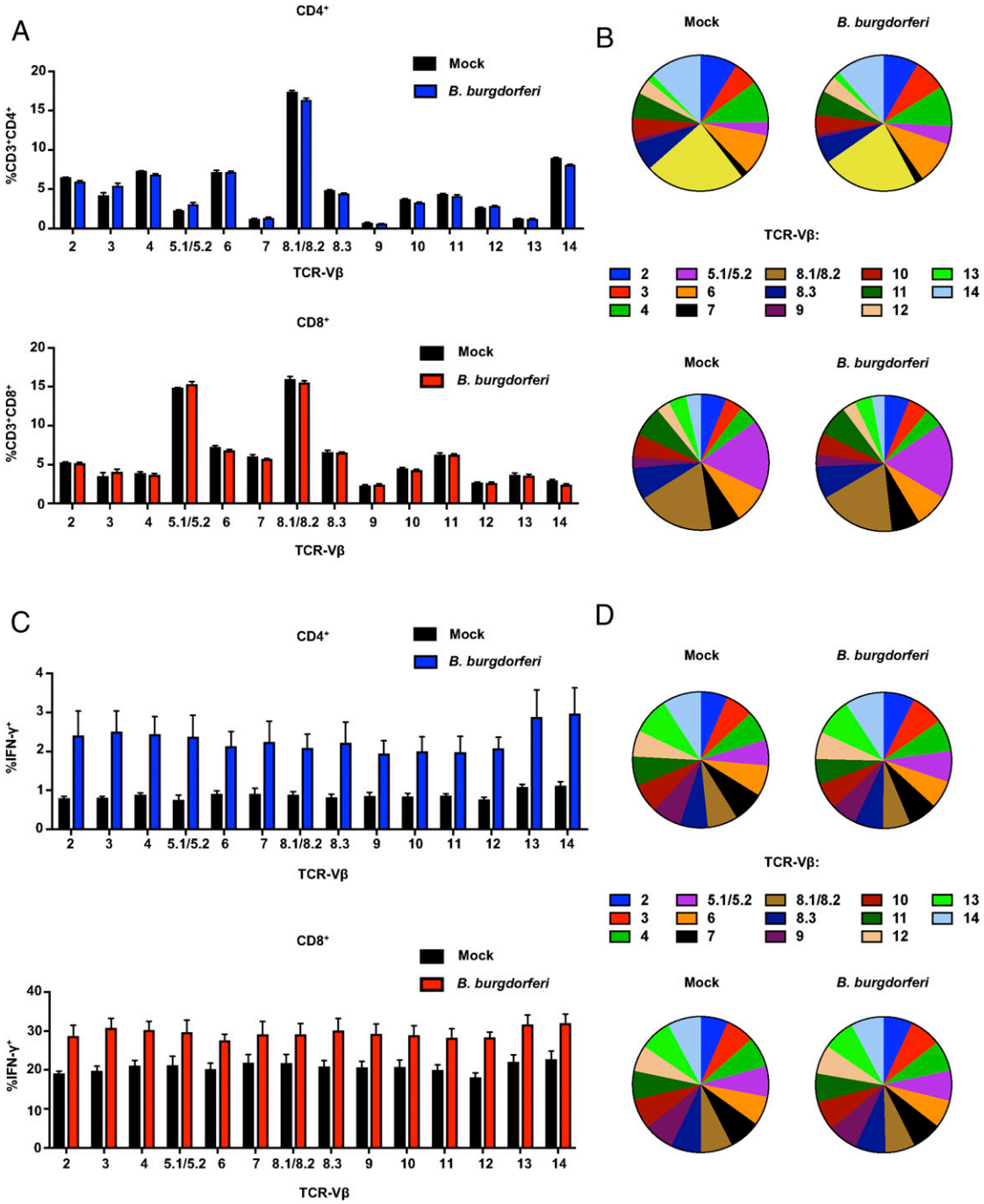

FIGURE 3. *B. burgdorferi* infection results in universal expansion and activation of $CD4^+$ and $CD8^+$ T cells. IL-$10^{-/-}$ mice were infected with *B. burgdorferi* for 4 wk, after which popliteal and inguinal lymph nodes were collected for analysis of TCR repertoires. (**A** and **B**) Frequency of TCR Vβ–specific cells was quantified for $CD3^+CD4^+$ (upper panel) or $CD3^+CD8^+$ (lower panel) gated populations. (**C** and **D**) Frequency of TCR Vβ–specific cells was quantified for $CD4^+$IFN-γ^+ (upper panel) and $CD8^+$IFN-γ^+ (lower panel) gated populations. Error bars indicate the SEM ($n \geq 3$ per group). Data are representative of two independent experiments.

sacrifice in the draining lymph nodes and the joints and determined to be >95% effective (Supplemental Fig. 2A–C). Arthritis severity in mice receiving anti-CD4 Ab was similar to mice receiving isotype control, whereas neutralization of CD8 partially reduced arthritis (Fig. 2A). The neutralization of both CD4 and CD8 reduced ankle swelling and histopathology scores (Fig. 2A, 2B). Mice that were treated with anti-CD4 displayed an increase in bacterial burden in joint tissue as compared with isotype control–treated animals (Fig. 2C), which is consistent with previous studies (54). Interestingly, $CD4^+$ T cells play a role in host defense not shared by $CD8^+$ T cells, as mice treated with anti-CD8 did not display an increase in bacterial burden in joint tissue (Fig. 2C). *B. burgdorferi*–infected IL-$10^{-/-}$ mice expressed transcripts for *Ifng*, *Cxcl9*, and *Cxcl10* in joint tissue that was significantly reduced only in mice treated with a combination of anti-CD4 and anti-CD8 (Fig. 2D–F). These data indicate that both $CD4^+$ and $CD8^+$ T cells contribute the expression of IFN-γ and IFN-γ–dependent genes in the joints of *B. burgdorferi*–infected mice. In the absence of $CD4^+$ T cells, the number of $CD8^+$IFN-γ^+ T cells increased substantially, suggesting that $CD8^+$ T cells are able to compensate for the loss of $CD4^+$-derived IFN-γ (Supplemental Fig. 2D). The number of $CD4^+$IFN-γ^+ T cells also increased in

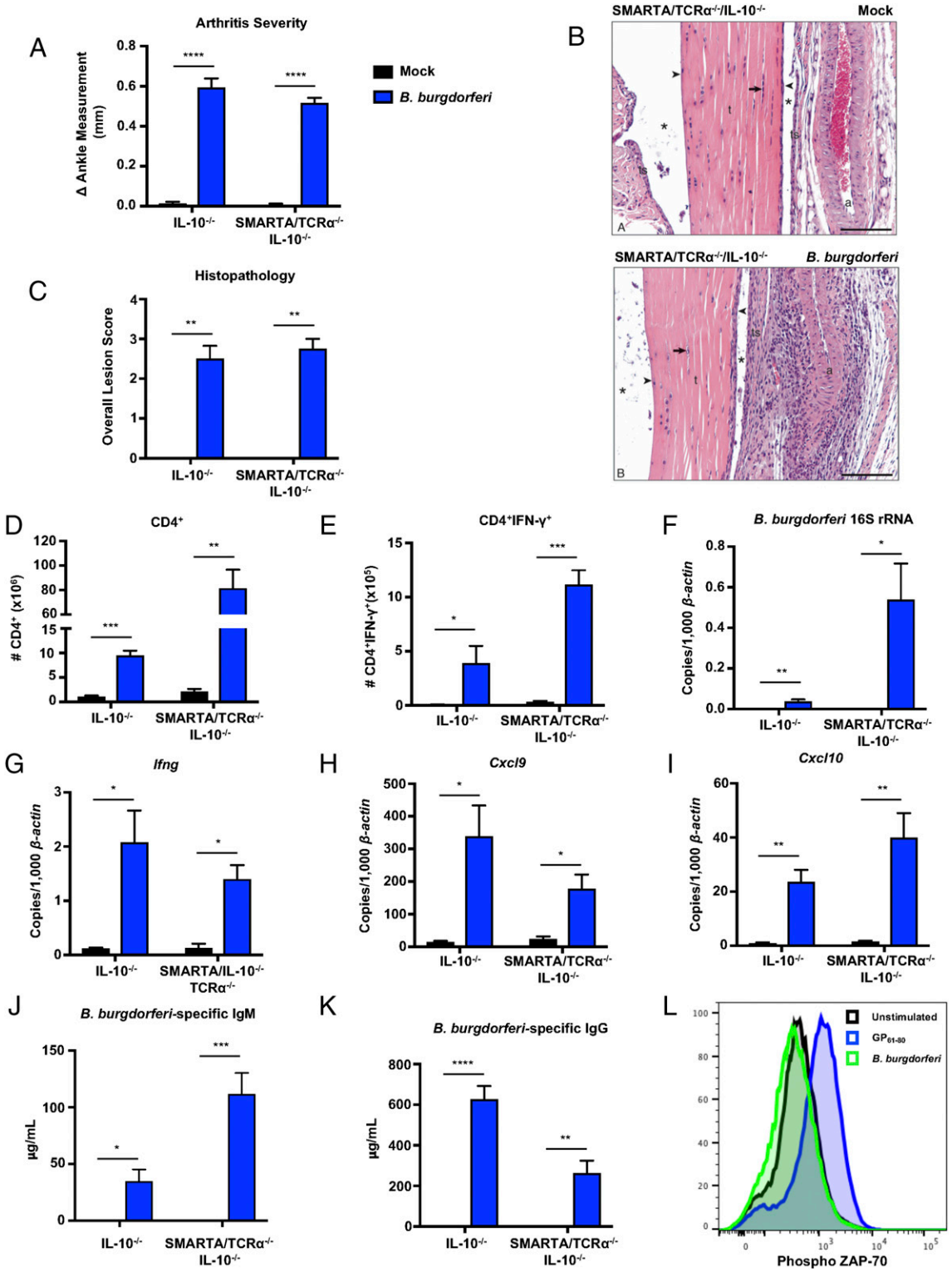

FIGURE 4. *B. burgdorferi* infection results in Ag-independent expansion and activation of TCR transgenic CD4$^+$ T cells. IL-10$^{-/-}$ and CD4$^+$ TCR transgenic SMARTA/TCRα$^{-/-}$/IL-10$^{-/-}$ mice were infected with *B. burgdorferi* for 4 wk. (**A**) Measurements of rear ankles of mice were taken before infection and 4 wk postinfection, and change in ankle measurement is shown. (**B**) Representative images of H&E-stained tibiotarsal joints from mock-infected (control) and 4 wk-infected SMARTA/TCRα$^{-/-}$/IL-10$^{-/-}$ mice used for histopathology scoring. *, tendon space; a, arteriole; t, tendon; ts, tendon sheath. Arrows point to tenocytes; arrowheads point to synoviocytes. Scale bars, 100 μm. (**C**) The most swollen ankle was subjected to blinded histopathologic evaluation in a blind fashion. Scores of 0–5, with 5 being most severe, were assigned to each sample. (**D**) The total number of CD4$^+$ T cells were quantified from the popliteal and inguinal lymph nodes. (**E**) Lymph node cells were stimulated with PMA/ionomycin in presence of brefeldin A, and the numbers of CD4$^+$IFN-γ$^+$ T cells were quantified using flow cytometry. (**F–I**) Quantification of *B. burgdorferi*–specific *16S rRNA*, *Ifng*, *Cxcl9*, and *Cxcl10* was normalized to 1000 *β-actin* in the joint using qRT-PCR. (**J** and **K**) Serum was obtained from mice 2 wk postinfection and assessed for *B. burgdorferi*–specific IgM (J) and *B. burgdorferi*–specific IgG (K) using sonicated *B. burgdorferi* bound to ELISA plates (see *Materials and Methods*). (**L**) Unfractionated naive SMARTA/TCRα$^{-/-}$/IL-10$^{-/-}$ splenocytes were isolated and stimulated in the presence of *B. burgdorferi* (10 μg/ml) or $gp_{61–80}$ (1 μM) for 3 h. SMARTA CD4$^+$ T cells were analyzed by flow cytometry for phosphorylated ZAP-70. Error bars indicate the *(Figure legend continues)*

the absence of $CD8^+$ T cells. Taken together, these data demonstrate that $CD4^+$ and $CD8^+$ T cells act synergistically to drive Lyme arthritis. These findings additionally highlight the lack of correlation between the bacterial burden of *B. burgdorferi* and the development of arthritis.

B. burgdorferi *infection results in universal expansion and activation of $CD4^+$ and $CD8^+$ T cells*

We next explored the possibility that T cells were being activated in a manner independent of classical TCR-mediated recognition. To address this possibility, the relative distribution of 14 different TCR β-chain V region (Vβ) subsets were examined in T cells from draining lymph nodes of *B. burgdorferi*–infected IL-$10^{-/-}$ mice using a TCR Vβ repertoire panel (BD Biosciences). TCR Vβ profiling is a standard assay routinely used in our laboratory (55, 56), and Ag-specific T cell activation results in population skewing toward a few selected TCR Vβ families. Stimulation of WT C57BL/6 lymph node cells with the immunodominant glycoprotein, $gp_{61–80}$, from LCMV results in expansion of TCR Vβ 8.3 (data not shown). In contrast, bystander T cell responses involve a wide diversity of TCRs, suggesting Ag-independent activation (57). IL-$10^{-/-}$ mice displayed increased numbers of $CD4^+$ and $CD8^+$ T cells in the draining lymph nodes during *B. burgdorferi* infection (Fig. 3A, Supplemental Fig. 1). However, there was no selective expansion of any individual Vβ subset on either $CD4^+$ or $CD8^+$ T cells during *B. burgdorferi* infection, which is indicative of a polyclonal or nonspecific T cell response. (Fig. 3B, 3C). Similarly, we did not observe any change in the frequency of IFN-γ–producing cells among TCR Vβ subsets following infection (Fig. 3C). These results support the hypothesis that T cell expansion in the draining lymph nodes during *B. burgdorferi* infection is independent of Ag specificity.

B. burgdorferi *infection results in Ag-independent expansion and activation of TCR transgenic $CD4^+$ T cells*

To directly confirm Ag-independent activation of $CD4^+$ T cells, TCR transgenic SMARTA mice were used. SMARTA mice possess $CD4^+$ T cells with monoclonal specificity for the MHC class II–restricted epitope of LCMV $gp_{61–80}$. This epitope is not found in *B. burgdorferi*, and thus SMARTA $CD4^+$ T cells cannot not become activated through TCR engagement during *B. burgdorferi* infection. To determine whether Ag-independent activation was occurring during *B. burgdorferi* infection, SMARTA mice were crossed to IL-$10^{-/-}$ mice to generate TCR transgenic SMARTA/IL-$10^{-/-}$ mice (see *Materials and Methods*). To further eliminate the possibility that residual non-SMARTA TCRs (present on ~5% of T cells) or dual TCRs on SMARTA T cells could recognize *B. burgdorferi* Ags, the SMARTA/IL-$10^{-/-}$ mice were further crossed to a TCR$\alpha^{-/-}$ background (SMARTA/TCR$\alpha^{-/-}$/IL-$10^{-/-}$).

SMARTA/TCR$\alpha^{-/-}$/IL-$10^{-/-}$mice and IL-$10^{-/-}$ were infected with *B. burgdorferi* and sacrificed 4 wk postinfection. SMARTA/TCR$\alpha^{-/-}$/IL-$10^{-/-}$mice developed severe arthritis and histopathologic lesions, suggesting that *B. burgdorferi*–specific T cells are not responsible for arthritis development (Fig. 4A, 4B). Further histopathologic analysis of infected SMARTA/TCR$\alpha^{-/-}$/IL-$10^{-/-}$mice revealed that the tendon sheath is reactive and thickened. Synoviocytes (arrowheads) covering the tendon and lining the tendon sheath are reactive and increased in number and size. Adjacent supporting stroma (extracellular matrix) under the tendon sheath is also thickened and contains neutrophils (subacute inflammation) admixed with lymphocytes and occasional macrophages (i.e., mononuclear inflammatory cells) as well as immature fibroblasts and collagen fibers (Fig. 4B). Examination of the draining lymph nodes from *B. burgdorferi*–infected SMARTA/TCR$\alpha^{-/-}$/IL-$10^{-/-}$ mice revealed an increase in $CD4^+$ T cells compared with mock-infected controls, indicating expansion of TCR transgenic T cells (Fig. 4D). Additionally, the number of $CD4^+$IFN-γ^+ T cells increased in *B. burgdorferi*–infected SMARTA/TCR$\alpha^{-/-}$/IL-$10^{-/-}$ mice, indicating that classical TCR recognition of *B. burgdorferi* Ag is not required for IFN-γ secretion by $CD4^+$ T cells (Fig. 4E). Concentrations of *B. burgdorferi 16S rRNA* were observed in the joint tissue of SMARTA/TCR$\alpha^{-/-}$/IL-$10^{-/-}$ mice (Fig. 4F). Joint tissue was also analyzed for the presence of *Ifng*, *Cxcl9*, and *Cxcl10* transcripts, all of which were elevated in infected SMARTA/TCR$\alpha^{-/-}$/IL-$10^{-/-}$ mice compared with mock-infected controls (Fig. 4G–I). We observed an increase in *B. burgdorferi*–specific IgM and a decrease in *B. burgdorferi*–specific IgG in infected SMARTA/TCR$\alpha^{-/-}$/IL-$10^{-/-}$mice compared with IL-$10^{-/-}$ mice (Fig. 4J, 4K), suggesting that there is a lack of T cell help for class switching. To confirm that there were no cross-reactive Ags present in *B. burgdorferi*, phosphorylation of the direct substrate of TCR activation, ZAP-70, was assayed. SMARTA/TCR$\alpha^{-/-}$/IL-$10^{-/-}$ $CD4^+$ T cells displayed increased phosphorylation of ZAP-70 when stimulated with their cognate Ag, $gp_{61–80}$. However, when stimulated with *B. burgdorferi*, there was no phosphorylation of ZAP-70, indicating that TCR signaling is not occurring (Fig. 4L). It has been previously shown that neutralization of IFN-γ in infected IL-$10^{-/-}$ mice significantly reduced ankle swelling and histopathology scores (38). IFN-γ neutralization in infected SMARTA/TCR$\alpha^{-/-}$/IL-$10^{-/-}$mice also resulted in a significant decrease in arthritis severity and histopathology scores (Supplemental Fig. 3A, 3B). However, arthritis was still elevated above mock-infected animals, indicating that other components are also contributing to arthritis. Interestingly, IFN-γ neutralization did not affect expansion of SMARTA/TCR$\alpha^{-/-}$/IL-$10^{-/-}$ $CD4^+$ T cells in the draining lymph nodes (Supplemental Fig. 3C) but resulted in decreased expression of *Ifng*, *Cxcl9*, and *Cxcl10* in joint tissue, providing further support that IFN-γ influences arthritis development upon *B. burgdorferi* infection in $CD4^+$ transgenic mice (Supplemental Fig. 3E–G). Overall, these data demonstrate that *B. burgdorferi* infection results in Ag-independent expansion and activation of $CD4^+$ T cells in the draining lymph node, resulting in the development of arthritis.

B. burgdorferi *infection of $CD8^+$ TCR transgenic mice results in arthritis and IFN-γ production*

To determine whether $CD8^+$ T cells were contributing to the development of Lyme arthritis in an Ag-independent mechanism, TCR transgenic Rag2$^{-/-}$/OT-I mice were used. Rag2$^{-/-}$/OT-I mice possess $CD8^+$ T cells with monoclonal specificity to chicken OVA-derived MHC class I–restricted epitope $OVA_{257–264}$. Rag2$^{-/-}$/OT-I mice were crossed to IL-$10^{-/-}$ mice to generate OT-I/Rag2$^{-/-}$/IL-$10^{-/-}$ mice. OT-I/Rag2$^{-/-}$/IL-$10^{-/-}$ and IL-$10^{-/-}$ mice were infected with *B. burgdorferi* and sacrificed 4 wk postinfection. OT-I/Rag2$^{-/-}$/IL-$10^{-/-}$ mice developed severe arthritis and histopathologic lesions similar to

SEM ($n \geq 8$ per group). Data are representative of two independent experiments. Significant differences between mock and *B. burgdorferi*–infected groups for each genotype were determined by a Student *t* test, with a Mann–Whitney *U* test used for categorically accessed lesion scores (C) (*$p < 0.05$, **$p < 0.01$, ***$p < 0.001$, ****$p < 0.0001$).

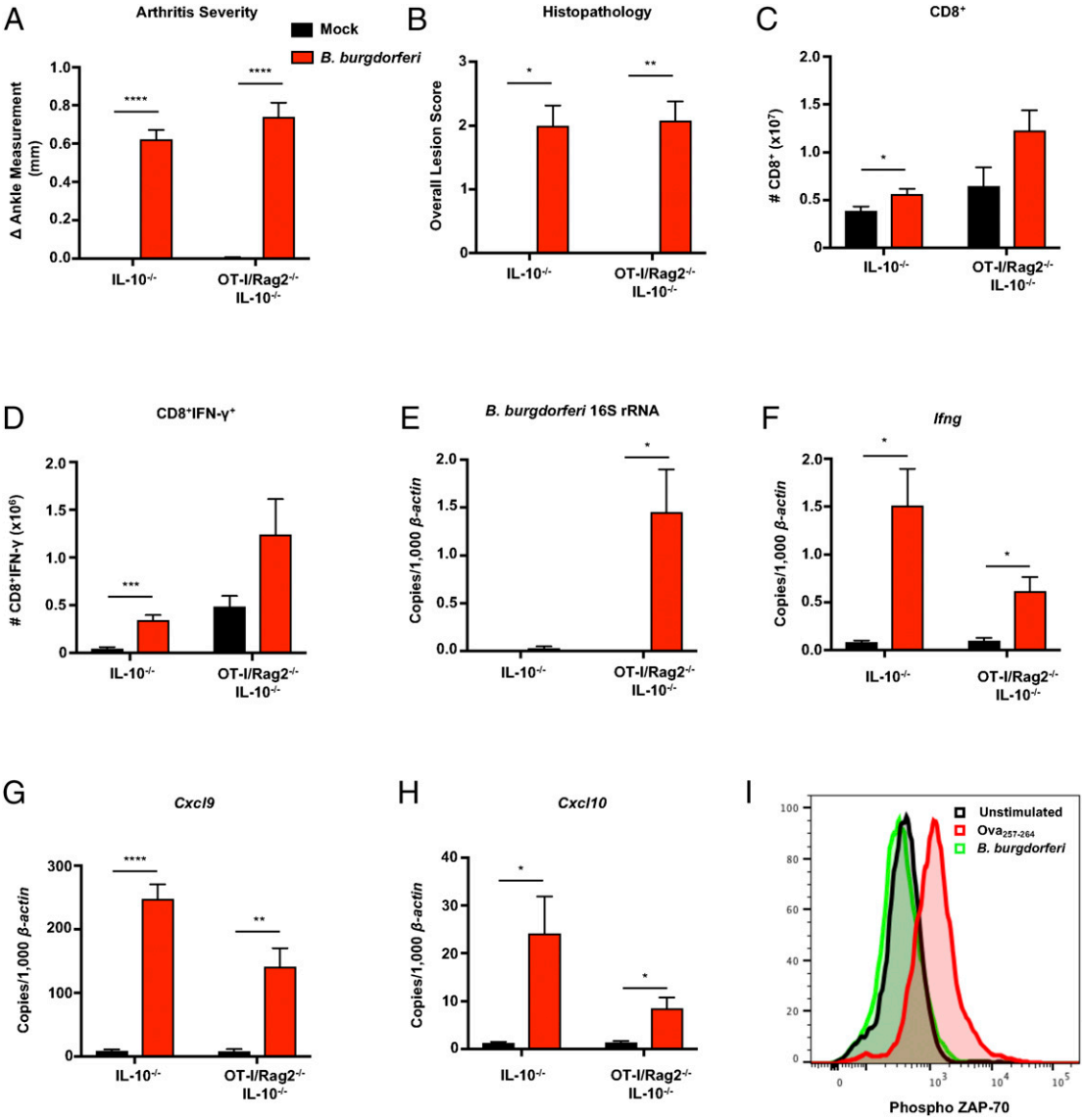

FIGURE 5. *B. burgdorferi* infection of CD8$^+$ TCR transgenic mice results in arthritis and IFN-γ production. IL-10$^{-/-}$ and CD8$^+$ TCR transgenic OT-I/Rag2$^{-/-}$/IL-10$^{-/-}$ mice were infected with *B. burgdorferi* for 4 wk. (**A**) Rear ankles of mice were measured before infection and 4 wk postinfection, and change in ankle measurement is shown. (**B**) The most swollen ankle was subjected to histopathologic evaluation in a blinded fashion. Scores of 0–5, with 5 being most severe, were assigned to each sample. (**C**) The total number of CD8$^+$ were quantified from the popliteal and inguinal lymph nodes. (**D**) Lymph node cells were stimulated with PMA/ionomycin in the presence of brefeldin A, and the numbers of CD8$^+$IFN-γ$^+$ T cells were quantified using flow cytometry. (**E**–**H**) Quantification of *B. burgdorferi*–specific *16S rRNA*, *Ifng*, *Cxcl9*, and *Cxcl10* was normalized to 1000 *β-actin* in the joint using qRT-PCR. (**I**) Unfractionated naive OT-I/Rag2$^{-/-}$/IL-10$^{-/-}$ splenocytes were isolated and stimulated in the presence of *B. burgdorferi* (10 μg/ml) or OVA$_{257–264}$ (1 μM) for 3 h. OT-I CD8$^+$ T cells were analyzed by flow cytometry for phosphorylated ZAP-70. Error bars indicate the SEM ($n \geq 5$ per group). Data are representative of two independent experiments. Significant differences between infected and uninfected groups for each genotype are indicated by a Student *t* test (*$p < 0.05$, **$p < 0.01$). For lesion scoring, a Mann–Whitney *U* test was used to determine statistically significant differences with groups, with *p* values indicated.

IL-10$^{-/-}$ mice (Fig. 5A, 5B). Examination of the draining lymph nodes revealed a trending increase in CD8$^+$ T cells from OT-I/Rag2$^{-/-}$/IL-10$^{-/-}$ mice compared with mock-infected controls (Fig. 5C), similar to CD8$^+$ T cells in the IL-10$^{-/-}$ experimental group included for comparison (Fig. 5C). Additionally, there was a trending increase in CD8$^+$IFN-γ$^+$ T cells in the lymph nodes of OT-I/Rag2$^{-/-}$/IL-10$^{-/-}$ compared with mock-infected controls, indicating that CD8$^+$ T cells are capable of producing IFN-γ following *Borrelia*-induced bystander activation (Fig. 5D). We observed concentrations of *B. burgdorferi 16S rRNA* in the joints of OT-I/Rag2$^{-/-}$/IL-10$^{-/-}$ mice, likely due to the absence of B cells (Fig. 5E). There was also a similar type II IFN profile observed in joint tissues, as *Ifng*, *Cxcl9*, and *Cxcl10* transcripts were all elevated in *B. burgdorferi*–infected OT-I/Rag2$^{-/-}$/IL-10$^{-/-}$ mice as compared with mock-infected controls (Fig. 5F–H). The use of a second TCR transgenic mouse that consists of CD8$^+$ T cells recognizing a different Ag (OVA) further addresses the unlikely possibility of a cross-reactive *Borrelia* epitope. Phosphorylation of ZAP-70 did not occur when OT-I CD8$^+$ T cells were stimulated with *B. burgdorferi*, indicating that T cell activation was not occurring through the TCR (Fig. 5I). Similar to the observations made for CD4$^+$ T cells, these results indicate that CD8$^+$ T cell activation and IFN-γ production occur via bystander activation during *B. burgdorferi*–induced arthritis. Overall, our results indicate a critical role for bystander T cell activation in mediating IFN-γ–dependent Lyme arthritis.

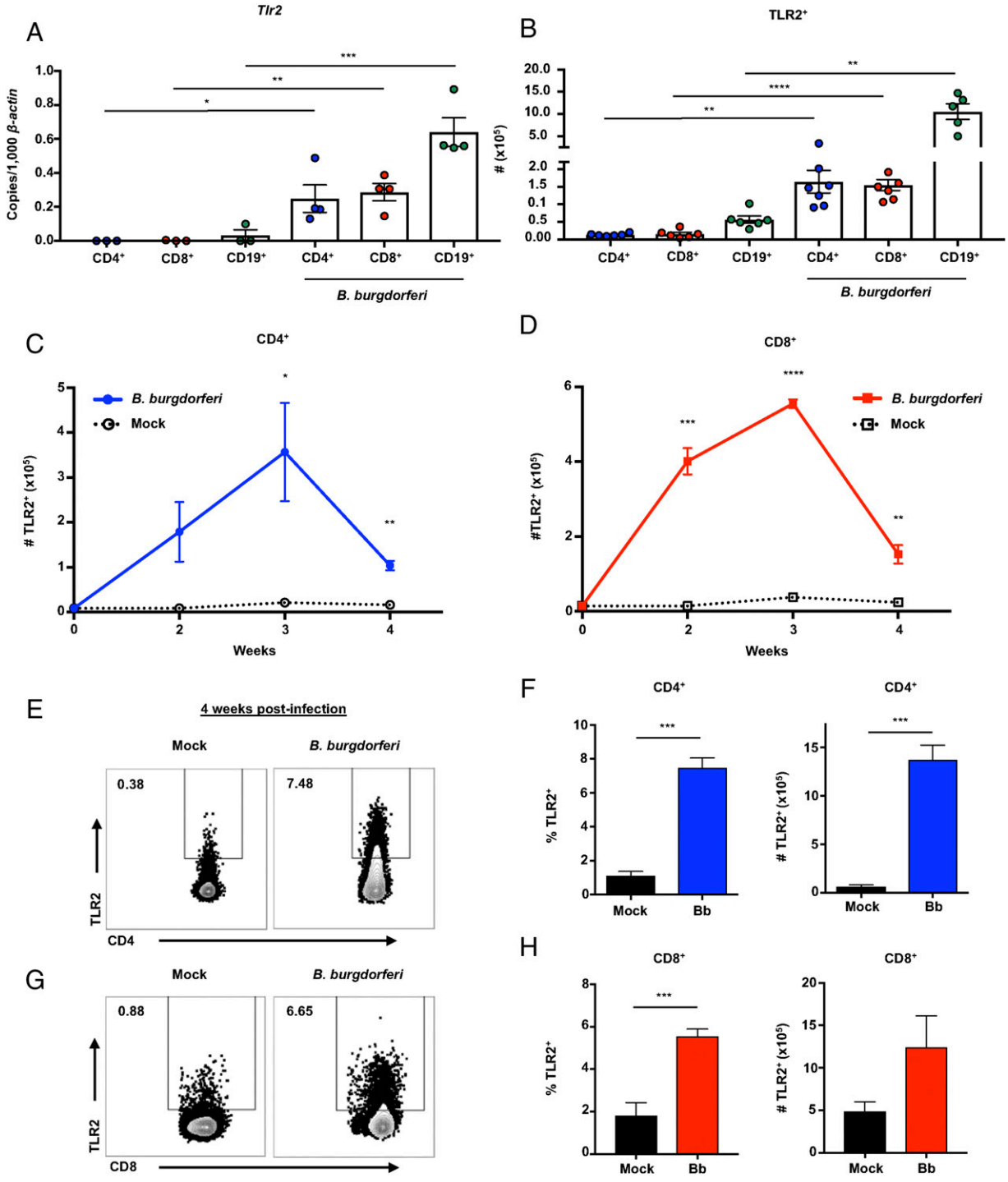

FIGURE 6. T cells display increased transcription and expression of TLR2 following *B. burgdorferi* infection. Mice were infected with *B. burgdorferi*, after which popliteal and inguinal lymph nodes were collected for analysis of T cells and TLR2 expression. (**A**) $CD3^+CD4^+$, $CD3^+CD8^+$, and $CD19^+$ cells were sorted from popliteal and inguinal lymph nodes of IL-$10^{-/-}$ mice using FACS sorting (BD FACSAria) 2 wk postinfection. *Tlr2* transcripts were measured in each cell population by qRT-PCR and normalized to 1000 *β-actin*. (**B**) Quantification of the total number of $CD3^+CD4^+TLR2^+$ and $CD3^+CD8^+$ $TLR2^+$ cells from IL-$10^{-/-}$ were determined by flow cytometry 4 wk postinfection. (**C** and **D**) IL-$10^{-/-}$ mice were sacrificed at 1 wk time intervals and analyzed by flow cytometry for TLR2 expression on $CD3^+CD4^+$ T cells (C) and $CD3^+CD8^+$ T cells (D). (**E** and **F**) SMARTA/TCR$\alpha^{-/-}$/IL-$10^{-/-}$ mice were infected with *B. burgdorferi* for 4 wk, after which popliteal and inguinal lymph nodes were collected for analysis of T cells and TLR2 expression. (E) Numbers in upper left corner of flow plots are percentage $TLR2^+$ cells. (F) The frequency and total number of $CD3^+CD4^+TLR2^+$ cells were determined by flow cytometry. (**G** and **H**) OT-I/Rag2$^{-/-}$/IL-$10^{-/-}$ mice were infected with *B. burgdorferi* for 4 wk, after which popliteal and inguinal lymph nodes were collected for analysis of T cells and TLR2 expression. (G) Numbers in the upper left corner of flow plots are percentage $TLR2^+$ cells. (H) Quantification of the frequency and total number of $CD3^+CD8^+TLR2^+$ cells were determined by flow cytometry. Error bars indicate the SEM ($n \geq 3$ per group). Data are representative of two independent experiments. $^*p < 0.05$, $^{**}p < 0.01$, $^{***}p < 0.001$, $^{****}p < 0.0001$, between infected and uninfected groups by a Student *t* test.

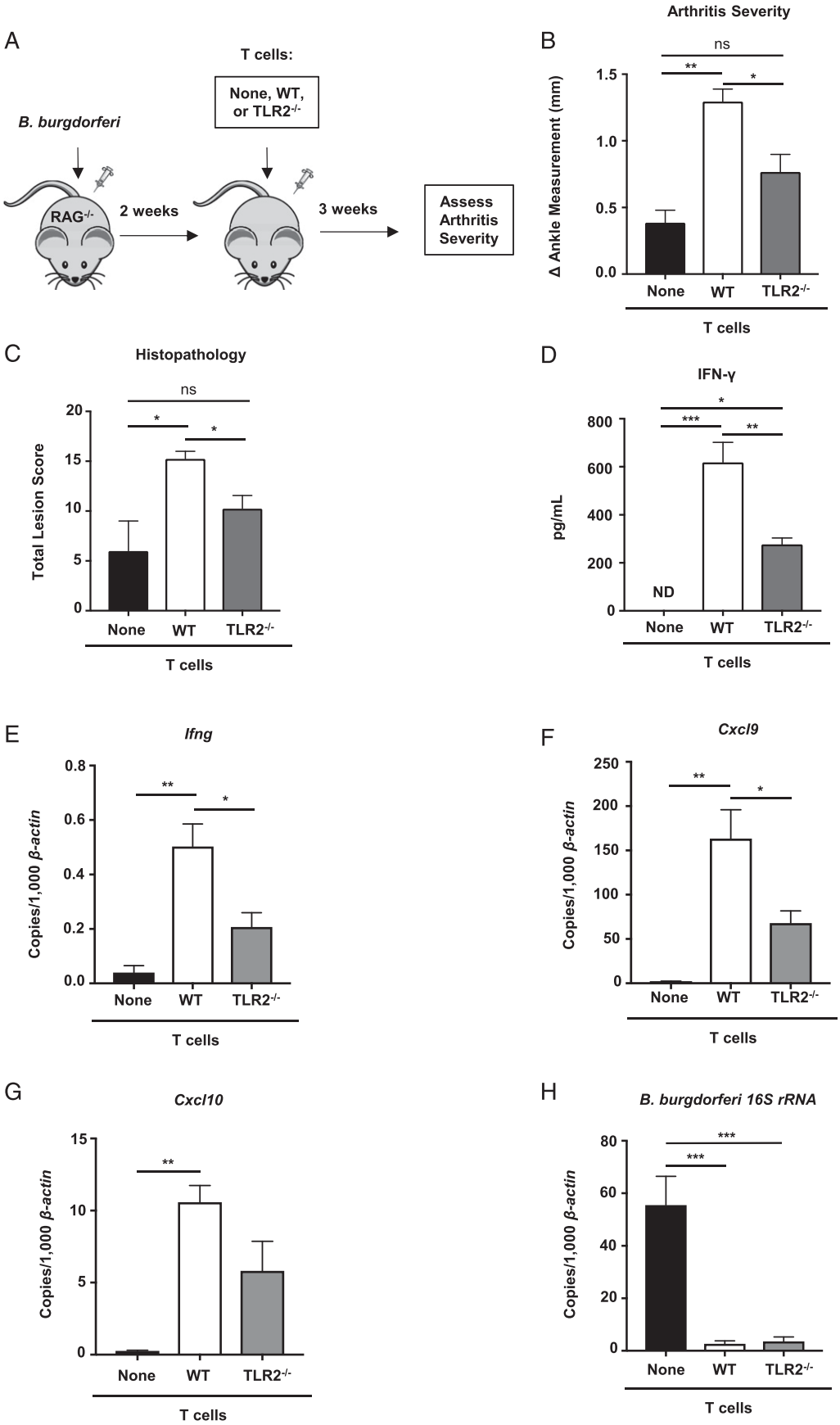

FIGURE 7. TLR2 expression on T cells enhances IFN-γ production and Lyme arthritis. (**A**) C57BL/6 Rag1$^{-/-}$ mice were infected with *B. burgdorferi* 2 wk before an i.v. injection of 6.5 × 10^6 T cells isolated from the popliteal and inguinal lymph nodes and spleens of naive healthy C57BL/6 WT or TLR2$^{-/-}$ mice. Infected Rag1$^{-/-}$ mice that did not receive lymphocytes served as controls. (**B**) Arthritis severity was determined 5 wk after infection (3 wk after injection of T cells). (**C**) The most swollen ankle was assessed by histopathologic evaluation in a blinded fashion. *(Figure legend continues)*

Lyme arthritis results in increased transcription and expression of TLR2 on CD4$^+$ and CD8$^+$ T cells

B. burgdorferi possess lipoproteins with a potent ability to stimulate host pathogen recognition receptors such as TLRs. TLR2 has been implicated as an important player in host defense, as TLR2$^{-/-}$ mice experience deficiencies in clearing *B. burgdorferi* and harbor more bacteria in the joints compared with WT mice (25, 26). It has recently been appreciated that both CD4$^+$ and CD8$^+$ T cells are capable of expressing TLR2 (29, 58). To evaluate the expression of TLR2 on T cells during *B. burgdorferi* infection, flow cytometry and qRT-PCR were performed on cells from the draining lymph nodes of infected IL-10$^{-/-}$ mice. Draining lymph nodes were collected 2 wk postinfection and CD4$^+$, CD8$^+$, and CD19$^+$ cells were isolated by flow cytometry. *Tlr2* transcripts were significantly elevated in both T and B cells following *B. burgdorferi* infection (Fig. 6A). The increase of *Tlr2* transcript was specific, as *Tlr1*, *Tlr6*, *Tlr7*, and *Tlr9* transcripts remained unchanged (Supplemental Fig. 4). At peak arthritis severity, the total number of CD4$^+$ and CD8$^+$ T cells expressing TLR2 protein had increased ~10-fold compared with mock-infected mice, indicating the potent ability of *B. burgdorferi* to upregulate TLR2 on T cells (Fig. 6B). The expression of TLR2 on both CD4$^+$ and CD8$^+$ T cells increased and peaked at 3 wk postinfection (Fig. 6C, 6D). This finding also coincided with the highest number of CD4$^+$IFN-γ$^+$ and CD8$^+$IFN-γ$^+$ T cells in the draining lymph node (Fig. 1D). To determine whether this occurred in the absence of a *B. burgdorferi*–specific TCR, we analyzed the expression of TLR2 in both SMARTA/TCRα$^{-/-}$/IL-10$^{-/-}$ and OT-I/Rag2$^{-/-}$/IL-10$^{-/-}$ mice. TLR2 expression was increased on both CD4$^+$ and CD8$^+$ TCR transgenic T cells upon *B. burgdorferi* infection as evidenced by the increase in frequency and total number of TLR2$^+$ T cells (Fig. 6E–H). These results indicate that *B. burgdorferi* infection leads to increased transcription and expression of TLR2 on both CD4$^+$ and CD8$^+$ T cells, and could play a role in T cell activation.

TLR2 expression on T cells enhances IFN-γ production and Lyme arthritis

The observation of *B. burgdorferi*–induced TLR2 expression on T cells prompted us to directly assess its role in arthritis development. C57BL/6 Rag1$^{-/-}$ mice were infected with *B. burgdorferi* 2 wk prior to an i.v. injection of T cells isolated from the lymph nodes and spleens of healthy naive WT or TLR2$^{-/-}$ C57BL/6 mice in a method described previously (19). In this experiment donor and recipient mice expressed IL-10. Infected Rag1$^{-/-}$ mice that did not receive T cells served as controls and had mild arthritis at 5 wk postinfection (Fig. 7A, 7B). Rag1$^{-/-}$ mice reconstituted with WT T cells developed severe arthritis compared with controls. Strikingly, mice that had received TLR2$^{-/-}$ T cells were protected from severe arthritis as measured by ankle swelling and histopathology scores (Fig. 7B, 7C). Mice that had received WT T cells had a significant increase in serum IFN-γ compared with mice receiving TLR2$^{-/-}$ T cells. There was no IFN-γ in the serum of mice that were not reconstituted with T cells (Fig. 7D). Furthermore, mice that had received WT T cells displayed an increase in *Ifng*, *Cxcl9*, and *Cxcl10* transcripts in the joint compared with mice reconstituted with TLR2$^{-/-}$ T cells (Fig. 7E–G). IFN-γ was still present in the serum and joints of mice receiving TLR2$^{-/-}$ T cells, indicating that other receptors for microbial patterns could contribute to the IFN-γ profile and the development of arthritis. It is also possible that other cytokines could also be contributing to bystander activation of T cells. Interestingly, the presence of either WT or TLR2$^{-/-}$ T cells drastically reduced the bacterial burden in the joint (Fig. 7F), suggesting that T cells play a role in enhancing host defense independent of TLR2. Taken together, these data reveal TLR2 as a critical mediator of T cell activation following *B. burgdorferi* infection, which results in enhanced IFN-γ production and Lyme arthritis.

Discussion

We conclude that persistent Lyme arthritis can be initiated and sustained through bystander activation of both CD4$^+$ and CD8$^+$ T cells. This is consistent with the absence of selective expansion of any individual Vβ subset on either CD4$^+$ or CD8$^+$ T cells during *B. burgdorferi* infection. Furthermore, Ag-independent expansion and activation of TCR transgenic CD4$^+$ or CD8$^+$ T cells was sufficient to induce arthritis. *B. burgdorferi* sequentially expresses an abundance of lipoproteins that are critical in the activation of TLR2 expressed by innate immune cells. We now demonstrate that *B. burgdorferi* induces TLR2 expression on T cells, which results in increased T cell activation and arthritis development. To our knowledge, this is the first example of CD4$^+$ T cells or CD8$^+$ T cells promoting arthritis pathogenesis in a TCR-independent mechanism.

Dysregulated immune responses are thought to play a key role in the pathogenesis of arthritis development. For example, Lyme disease patients with persisting symptoms after completing the standard dose of antibiotics often have lower frequencies of regulatory T cells and higher expression of coactivation receptors in their synovial fluid (30). This suggests that an inappropriately amplified immune response is contributing to arthritis development. Other studies have shown that chronic states of inflammation involving both systemic and local production of proinflammatory cytokines such as TNF and IL-6 are required for the pathogenesis of rheumatoid arthritis (59, 60). These results suggest that future CD4$^+$ and CD8$^+$ T cell studies should focus on costimulatory signals known to influence T cell activation and their role in Lyme and other arthralgias.

The involvement of T cells in Lyme arthritis development and resolution has been debated. Several reports suggest that the adaptive immune response is not required for acute Lyme arthritis development in genetically susceptible mouse strains (C3H), as *scid* and *rag* mice, which lack both functional B and T cells, develop arthritis upon *B. burgdorferi* infection (51, 61). However, adoptive transfer of CD4$^+$ T cells into *rag* mice was shown to exacerbate the severity of Lyme arthritis, implicating a role for dysregulated T cells in Lyme disease (19). Efforts have been made to understand the protective and disease-promoting roles of the Ag-specific T cell response to *B. burgdorferi* (19, 33, 54). Initial studies suggested that T cell responses to a spirochetal epitope

Scores of 0–5, with 5 being most severe, were assigned to each sample. The total score shown is based on polymorphic (neutrophils) and/or mononuclear cell (lymphocytes/macrophages) infiltrates, tendon sheath thickness, and reactive/reparative responses affecting the joint. (**D**) Quantification of IFN-γ in the serum was determined using ELISA. (**E**–**H**) Quantification of *Ifng*, *Cxcl9*, *Cxcl10*, and *B. burgdorferi*–specific *16S rRNA* was normalized to 1000 *β-actin* in the joint using qRT-PCR. Error bars indicate the SEM ($n = 4$ per group). $*p < 0.05$, $**p < 0.01$, $***p < 0.001$, between groups by ANOVA followed by a Bonferroni post hoc test. For lesion scoring, a Mann–Whitney *U* test was used to determine whether there was statistically significant difference with groups, with *p* values indicated. ns, not significant.

were cross-reacting with a similar epitope of a self-protein, resulting in molecular mimicry and autoimmune-like pathology (62). In support of this autoimmunity hypothesis, specific HLA-DR alleles such as DRB1*0101 and DRB1*01 have been linked as genetic risk factors for the development of antibiotic refractory arthritis (63). Recent studies have also identified autoantigens that are capable of acting as T cell targets in patients with Lyme disease (13, 64–66). Bystander activation of T cells may provide an environment for autoimmune-mediated disease development. Previous studies have identified bystander activation of γδ T cells in synovial fluid of patients with persistent symptoms, which is dependent on TLR activation of myeloid cells (35, 36). The mechanism by which these T cells are activated has yet to be determined, and future studies are needed to identify the primary signals that promote bystander activation. Our studies clearly provide a potential scenario in which localized activation of bystander T cells could result in the expansion of clones recognizing self-antigens.

Ag-independent or bystander T cell activation was first demonstrated in virally infected mice, which resulted in expansion and proliferation of heterologous polyclonal T cells (67). More recent studies have begun to illuminate the mechanisms driving this TCR-independent expansion of T cells and have implicated certain proinflammatory cytokines such as IFN-γ, IL-12, IL-15, and IL-18 as capable of causing bystander activation of mucosal-associated variant T cells and memory $CD8^+$ T cells (68–72). However, less is known about the signals that initiate $CD4^+$ T cell bystander activation. The ability of both $CD4^+$ and $CD8^+$ T cell bystander activation to exacerbate Lyme arthritis is unique. The presence of $CD8^+$ T cells was sufficient to fully promote Lyme arthritis in IL-$10^{-/-}$ mice, despite the absence of $CD4^+$ T cells and B cells. $CD4^+$ T cells have a dual role in host pathogenesis and host defense in this model system, as bacterial burden in the joints was higher in the absence of $CD4^+$ T cells. Differences in bacterial load between IL-$10^{-/-}$ and CD4 TCR transgenic mice indicate that although a *Borrelia*-specific $CD4^+$ T cell response is required for clearance of *B. burgdorferi*, it is not required to promote arthritis severity. This finding is consistent with previous publications using other mouse strains that show that *Borrelia* load does not correlate with arthritis severity (73, 74). It was also revealed that $CD4^+$ T cells play a role in the generation of *B. burgdorferi*–specific Abs, as their absence during infection resulted in decreased *B. burgdorferi*–specific IgG. This unique host defense feature of $CD4^+$ T cells is not shared by $CD8^+$ T cells, and it implicates a role for $CD4^+$ T cell Ag specificity in promoting bacterial clearance. Our findings suggest that $CD8^+$ T cells could even provide a therapeutic target for control of inflammation without compromising the ability to clear infection.

Several studies have reported a costimulatory role for TLRs on $CD8^+$ T cells. TLR2 expression on $CD8^+$ T cells leads to a decreased activation threshold for costimulatory signals received by APCs (75). Our data support these results, as TLR2 expression increased on both $CD4^+$ and $CD8^+$ T cells during *B. burgdorferi* infection. The expression of TLR2 on T cells also coincided with the increase in IFN-γ^+ T cells, further suggesting that TLR2 is playing a direct role in IFN-γ secretion. Strikingly, arthritis severity was greatly reduced when TLR2 was selectively missing from T cells, revealing TLR2 as a critical component of bystander T cell activation driving arthritis. Accumulating evidence supports significant alterations in T cell TLR expression in patients with infectious diseases. For example, T cells from patients with chronic hepatitis C express higher transcript levels of several TLRs in $CD8^+$ T cells compared with healthy controls (76). More studies are needed to assess the effect of altered TLR expression on T cells and its contribution to pathogenesis and immune defense.

This study highlights the Ag-independent role of both $CD4^+$ and $CD8^+$ T cells in the development of Lyme arthritis. Importantly, several observations in the IL-$10^{-/-}$ mouse model are recapitulated in posttreatment Lyme disease patients (31, 32). Synovial tissue from patients contains elevated numbers of $CD4^+$ T cells, as well as elevated concentrations of IFN-γ, CXCL9, and CXCL10, compared with patients whose arthritis resolves after antibiotics. This is unique, as other mouse models have not allowed for the assessment of T cell contribution. Therefore, our study reveals a role for T cell–driven arthritis, providing insight into the pathogenic potential of inflammatory dysregulation in Lyme disease.

Acknowledgments

We acknowledge Stephanie Meek, Peter Pioli, Robert Lochhead, Tyson Chiaro, Dylan Beyer, and Garrison Asper for technical assistance, training, advice and manuscript review, as well as James Marvin and Tessa Galland from the University of Utah Flow Cytometry Core Facility for expertise and assistance.

Disclosures

The authors have no financial conflicts of interest.

References

1. Hu, L. T. 2016. Lyme disease. *Ann. Intern. Med.* 164: ITC65–ITC80.
2. Steere, A. C., R. T. Schoen, and E. Taylor. 1987. The clinical evolution of Lyme arthritis. *Ann. Intern. Med.* 107: 725–731.
3. Cimmino, M. A., G. L. Moggiana, M. Parisi, and S. Accardo. 1996. Treatment of Lyme arthritis. *Infection* 24: 91–93.
4. Steere, A. C., and S. M. Angelis. 2006. Therapy for Lyme arthritis: strategies for the treatment of antibiotic-refractory arthritis. *Arthritis Rheum.* 54: 3079–3086.
5. Wills, A. B., A. B. Spaulding, J. Adjemian, D. R. Prevots, S. P. Turk, C. Williams, and A. Marques. 2016. Long-term follow-up of patients with Lyme disease: longitudinal analysis of clinical and quality-of-life measures. *Clin. Infect. Dis.* 62: 1546–1551.
6. Nocton, J. J., F. Dressler, B. J. Rutledge, P. N. Rys, D. H. Persing, and A. C. Steere. 1994. Detection of *Borrelia burgdorferi* DNA by polymerase chain reaction in synovial fluid from patients with Lyme arthritis. *N. Engl. J. Med.* 330: 229–234.
7. Li, X., G. A. McHugh, N. Damle, V. K. Sikand, L. Glickstein, and A. C. Steere. 2011. Burden and viability of *Borrelia burgdorferi* in skin and joints of patients with erythema migrans or Lyme arthritis. *Arthritis Rheum.* 63: 2238–2247.
8. Radolf, J. 2005. Posttreatment chronic Lyme disease—what it is not. *J. Infect. Dis.* 192: 948–949.
9. Shen, S., J. J. Shin, K. Strle, G. McHugh, X. Li, L. J. Glickstein, E. E. Drouin, and A. C. Steere. 2010. Treg cell numbers and function in patients with antibiotic-refractory or antibiotic-responsive Lyme arthritis. *Arthritis Rheum.* 62: 2127–2137.
10. Gross, D. M., A. C. Steere, and B. T. Huber. 1998. T helper 1 response is dominant and localized to the synovial fluid in patients with Lyme arthritis. *J. Immunol.* 160: 1022–1028.
11. Yudoh, K., H. Matsuno, F. Nakazawa, T. Yonezawa, and T. Kimura. 2000. Reduced expression of the regulatory $CD4^+$ T cell subset is related to Th1/Th2 balance and disease severity in rheumatoid arthritis. *Arthritis Rheum.* 43: 617–627.
12. Steere, A. C., E. Dwyer, and R. Winchester. 1990. Association of chronic Lyme arthritis with HLA-DR4 and HLA-DR2 alleles. *N. Engl. J. Med.* 323: 219–223.
13. Pianta, A., E. E. Drouin, J. T. Crowley, S. Arvikar, K. Strle, C. E. Costello, and A. C. Steere. 2015. Annexin A2 is a target of autoimmune T and B cell responses associated with synovial fibroblast proliferation in patients with antibiotic-refractory Lyme arthritis. *Clin. Immunol.* 160: 336–341.
14. Steere, A. C., and L. Glickstein. 2004. Elucidation of Lyme arthritis. *Nat. Rev. Immunol.* 4: 143–152.
15. Girschick, H. J., H. I. Huppertz, H. Rüssmann, V. Krenn, and H. Karch. 1996. Intracellular persistence of *Borrelia burgdorferi* in human synovial cells. *Rheumatol. Int.* 16: 125–132.
16. Bockenstedt, L. K., D. G. Gonzalez, A. M. Haberman, and A. A. Belperron. 2012. Spirochete antigens persist near cartilage after murine Lyme borreliosis therapy. *J. Clin. Invest.* 122: 2652–2660.
17. Embers, M. E., S. W. Barthold, J. T. Borda, L. Bowers, L. Doyle, E. Hodzic, M. B. Jacobs, N. R. Hasenkampf, D. S. Martin, S. Narasimhan, et al. 2012. Persistence of *Borrelia burgdorferi* in rhesus macaques following antibiotic treatment of disseminated infection. [Published erratum appears in 2013 *PLoS One* 8.] *PLoS One* 7: e29914.
18. Geissmann, F., T. O. Cameron, S. Sidobre, N. Manlongat, M. Kronenberg, M. J. Briskin, M. L. Dustin, and D. R. Littman. 2005. Intravascular immune surveillance by $CXCR6^+$ NKT cells patrolling liver sinusoids. *PLoS Biol.* 3: e113.
19. McKisic, M. D., W. L. Redmond, and S. W. Barthold. 2000. Cutting edge: T cell-mediated pathology in murine Lyme borreliosis. *J. Immunol.* 164: 6096–6099.
20. Fraser, C. M., S. Casjens, W. M. Huang, G. G. Sutton, R. Clayton, R. Lathigra, O. White, K. A. Ketchum, R. Dodson, E. K. Hickey, et al. 1997. Genomic sequence of a Lyme disease spirochaete, *Borrelia burgdorferi*. *Nature* 390: 580–586.

21. Hirschfeld, M., C. J. Kirschning, R. Schwandner, H. Wesche, J. H. Weis, R. M. Wooten, and J. J. Weis. 1999. Cutting edge: inflammatory signaling by *Borrelia burgdorferi* lipoproteins is mediated by Toll-like receptor 2. *J. Immunol.* 163: 2382–2386.
22. Alexopoulou, L., V. Thomas, M. Schnare, Y. Lobet, J. Anguita, R. T. Schoen, R. Medzhitov, E. Fikrig, and R. A. Flavell. 2002. Hyporesponsiveness to vaccination with *Borrelia burgdorferi* OspA in humans and in TLR1- and TLR2-deficient mice. *Nat. Med.* 8: 878–884.
23. Radolf, J. D., M. J. Caimano, B. Stevenson, and L. T. Hu. 2012. Of ticks, mice and men: understanding the dual-host lifestyle of Lyme disease spirochaetes. *Nat. Rev. Microbiol.* 10: 87–99.
24. Fikrig, E., S. W. Barthold, F. S. Kantor, and R. A. Flavell. 1990. Protection of mice against the Lyme disease agent by immunizing with recombinant OspA. *Science* 250: 553–556.
25. Wooten, R. M., Y. Ma, R. A. Yoder, J. P. Brown, J. H. Weis, J. F. Zachary, C. J. Kirschning, and J. J. Weis. 2002. Toll-like receptor 2 is required for innate, but not acquired, host defense to *Borrelia burgdorferi*. *J. Immunol.* 168: 348–355.
26. Wang, X., Y. Ma, A. Yoder, H. Crandall, J. F. Zachary, R. S. Fujinami, J. H. Weis, and J. J. Weis. 2008. T cell infiltration is associated with increased Lyme arthritis in TLR2$^{-/-}$ mice. *FEMS Immunol. Med. Microbiol.* 52: 124–133.
27. Lasky, C. E., C. L. Pratt, K. A. Hilliard, J. L. Jones, and C. R. Brown. 2016. T cells exacerbate lyme borreliosis in TLR2-deficient mice. *Front. Immunol.* 7: 468.
28. Komai-Koma, M., L. Jones, G. S. Ogg, D. Xu, and F. Y. Liew. 2004. TLR2 is expressed on activated T cells as a costimulatory receptor. *Proc. Natl. Acad. Sci. USA* 101: 3029–3034.
29. Round, J. L., S. M. Lee, J. Li, G. Tran, B. Jabri, T. A. Chatila, and S. K. Mazmanian. 2011. The Toll-like receptor pathway establishes commensal gut colonization. *Science* 332: 974–977.
30. Abdollahi-Roodsaz, S., L. A. Joosten, M. I. Koenders, I. Devesa, M. F. Roelofs, T. R. Radstake, M. Heuvelmans-Jacobs, S. Akira, M. J. Nicklin, F. Ribeiro-Dias, and W. B. van den Berg. 2008. Stimulation of TLR2 and TLR4 differentially skews the balance of T cells in a mouse model of arthritis. *J. Clin. Invest.* 118: 205–216.
31. Vudattu, N. K., K. Strle, A. C. Steere, and E. E. Drouin. 2013. Dysregulation of CD4$^+$CD25^{high} T cells in the synovial fluid of patients with antibiotic-refractory Lyme arthritis. *Arthritis Rheum.* 65: 1643–1653.
32. Soloski, M. J., L. A. Crowder, L. J. Lahey, C. A. Wagner, W. H. Robinson, and J. N. Aucott. 2014. Serum inflammatory mediators as markers of human Lyme disease activity. *PLoS One* 9: e93243.
33. Kang, I., S. W. Barthold, D. H. Persing, and L. K. Bockenstedt. 1997. T-helper-cell cytokines in the early evolution of murine Lyme arthritis. *Infect. Immun.* 65: 3107–3111.
34. Matyniak, J. E., and S. L. Reiner. 1995. T helper phenotype and genetic susceptibility in experimental Lyme disease. *J. Exp. Med.* 181: 1251–1254.
35. Collins, C., C. Shi, J. Q. Russell, K. A. Fortner, and R. C. Budd. 2008. Activation of γδ T cells by *Borrelia burgdorferi* is indirect via a TLR- and caspase-dependent pathway. *J. Immunol.* 181: 2392–2398.
36. Vincent, M. S., K. Roessner, D. Lynch, D. Wilson, S. M. Cooper, J. Tschopp, L. H. Sigal, and R. C. Budd. 1996. Apoptosis of Fas^{high} CD4$^+$ synovial T cells by *Borrelia*-reactive Fas-ligand^{high} γδ T cells in Lyme arthritis. *J. Exp. Med.* 184: 2109–2117.
37. Vincent, M. S., K. Roessner, T. Sellati, C. D. Huston, L. H. Sigal, S. M. Behar, J. D. Radolf, and R. C. Budd. 1998. Lyme arthritis synovial γδ T cells respond to *Borrelia burgdorferi* lipoproteins and lipidated hexapeptides. *J. Immunol.* 161: 5762–5771.
38. Sonderegger, F. L., Y. Ma, H. Maylor-Hagan, J. Brewster, X. Huang, G. J. Spangrude, J. F. Zachary, J. H. Weis, and J. J. Weis. 2012. Localized production of IL-10 suppresses early inflammatory cell infiltration and subsequent development of IFN-γ–mediated Lyme arthritis. *J. Immunol.* 188: 1381–1393.
39. Lochhead, R. B., J. F. Zachary, L. Dalla Rosa, Y. Ma, J. H. Weis, R. M. O'Connell, and J. J. Weis. 2015. Antagonistic interplay between microRNA-155 and IL-10 during Lyme carditis and arthritis. *PLoS One* 10: e0135142.
40. Pianta, A., S. L. Arvikar, K. Strle, E. E. Drouin, Q. Wang, C. E. Costello, and A. C. Steere. 2017. Two rheumatoid arthritis–specific autoantigens correlate microbial immunity with autoimmune responses in joints. *J. Clin. Invest.* 127: 2946–2956.
41. Oxenius, A., M. F. Bachmann, R. M. Zinkernagel, and H. Hengartner. 1998. Virus-specific MHC class II-restricted TCR-transgenic mice: effects on humoral and cellular immune responses after viral infection. *Eur. J. Immunol.* 28: 390–400.
42. Liu, F., and J. L. Whitton. 2005. Cutting edge: re-evaluating the in vivo cytokine responses of CD8$^+$ T cells during primary and secondary viral infections. *J. Immunol.* 174: 5936–5940.
43. Lochhead, R. B., Y. Ma, J. F. Zachary, D. Baltimore, J. L. Zhao, J. H. Weis, R. M. O'Connell, and J. J. Weis. 2014. MicroRNA-146a provides feedback regulation of Lyme arthritis but not carditis during infection with *Borrelia burgdorferi*. *PLoS Pathog.* 10: e1004212.
44. Crandall, H., D. M. Dunn, Y. Ma, R. M. Wooten, J. F. Zachary, J. H. Weis, R. B. Weiss, and J. J. Weis. 2006. Gene expression profiling reveals unique pathways associated with differential severity of lyme arthritis. *J. Immunol.* 177: 7930–7942.
45. Ornstein, K., and A. G. Barbour. 2006. A reverse transcriptase-polymerase chain reaction assay of *Borrelia burgdorferi* 16S rRNA for highly sensitive quantification of pathogen load in a vector. *Vector Borne Zoonotic Dis.* 6: 103–112.
46. Miller, J. C., Y. Ma, J. Bian, K. C. Sheehan, J. F. Zachary, J. H. Weis, R. D. Schreiber, and J. J. Weis. 2008. A critical role for type I IFN in arthritis development following *Borrelia burgdorferi* infection of mice. *J. Immunol.* 181: 8492–8503.
47. Brown, J. P., J. F. Zachary, C. Teuscher, J. J. Weis, and R. M. Wooten. 1999. Dual role of interleukin-10 in murine Lyme disease: regulation of arthritis severity and host defense. *Infect. Immun.* 67: 5142–5150.
48. Strle, K., K. B. Sulka, A. Pianta, J. T. Crowley, S. L. Arvikar, A. Anselmo, R. Sadreyev, and A. C. Steere. 2017. T-helper 17 cell cytokine responses in Lyme disease correlate with *Borrelia burgdorferi* antibodies during early infection and with autoantibodies late in the illness in patients with antibiotic-refractory Lyme arthritis. *Clin. Infect. Dis.* 64: 930–938.
49. Arvikar, S. L., J. T. Crowley, K. B. Sulka, and A. C. Steere. 2017. Autoimmune arthritides, rheumatoid arthritis, psoriatic arthritis, or peripheral spondyloarthritis following Lyme disease. *Arthritis Rheumatol.* 69: 194–202.
50. Brown, C. R., and S. L. Reiner. 1999. Experimental lyme arthritis in the absence of interleukin-4 or γ interferon. *Infect. Immun.* 67: 3329–3333.
51. Barthold, S. W., C. L. Sidman, and A. L. Smith. 1992. Lyme borreliosis in genetically resistant and susceptible mice with severe combined immunodeficiency. *Am. J. Trop. Med. Hyg.* 47: 605–613.
52. Shin, J. J., L. J. Glickstein, and A. C. Steere. 2007. High levels of inflammatory chemokines and cytokines in joint fluid and synovial tissue throughout the course of antibiotic-refractory Lyme arthritis. *Arthritis Rheum.* 56: 1325–1335.
53. Glickstein, L., M. Edelstein, and J. Z. Dong. 2001. Gamma interferon is not required for arthritis resistance in the murine Lyme disease model. *Infect. Immun.* 69: 3737–3743.
54. Elsner, R. A., C. J. Hastey, and N. Baumgarth. 2015. CD4$^+$ T cells promote antibody production but not sustained affinity maturation during *Borrelia burgdorferi* infection. *Infect. Immun.* 83: 48–56.
55. Williams, M. A., E. V. Ravkov, and M. J. Bevan. 2008. Rapid culling of the CD4$^+$ T cell repertoire in the transition from effector to memory. *Immunity* 28: 533–545.
56. Kim, C., T. Wilson, K. F. Fischer, and M. A. Williams. 2013. Sustained interactions between T cell receptors and antigens promote the differentiation of CD4$^+$ memory T cells. *Immunity* 39: 508–520.
57. Horrocks, C., J. E. Holder, J. Berth-Jones, and R. D. Camp. 1997. Antigen-independent expansion of T cells from psoriatic skin lesions: phenotypic characterization and antigen reactivity. *Br. J. Dermatol.* 137: 331–338.
58. Reynolds, J. M., B. P. Pappu, J. Peng, G. J. Martinez, Y. Zhang, Y. Chung, L. Ma, X. O. Yang, R. I. Nurieva, Q. Tian, and C. Dong. 2010. Toll-like receptor 2 signaling in CD4$^+$ T lymphocytes promotes T helper 17 responses and regulates the pathogenesis of autoimmune disease. *Immunity* 32: 692–702.
59. Williams, R. O., M. Feldmann, and R. N. Maini. 1992. Anti-tumor necrosis factor ameliorates joint disease in murine collagen-induced arthritis. *Proc. Natl. Acad. Sci. USA* 89: 9784–9788.
60. Fujimoto, M., S. Serada, M. Mihara, Y. Uchiyama, H. Yoshida, N. Koike, Y. Ohsugi, T. Nishikawa, B. Ripley, A. Kimura, et al. 2008. Interleukin-6 blockade suppresses autoimmune arthritis in mice by the inhibition of inflammatory Th17 responses. *Arthritis Rheum.* 58: 3710–3719.
61. Brown, C. R., and S. L. Reiner. 1999. Genetic control of experimental lyme arthritis in the absence of specific immunity. *Infect. Immun.* 67: 1967–1973.
62. Gross, D. M., T. Forsthuber, M. Tary-Lehmann, C. Etling, K. Ito, Z. A. Nagy, J. A. Field, A. C. Steere, and B. T. Huber. 1998. Identification of LFA-1 as a candidate autoantigen in treatment-resistant Lyme arthritis. *Science* 281: 703–706.
63. Steere, A. C., W. Klitz, E. E. Drouin, B. A. Falk, W. W. Kwok, G. T. Nepom, and L. A. Baxter-Lowe. 2006. Antibiotic-refractory Lyme arthritis is associated with HLA-DR molecules that bind a *Borrelia burgdorferi* peptide. *J. Exp. Med.* 203: 961–971.
64. Drouin, E. E., R. J. Seward, K. Strle, G. McHugh, K. Katchar, D. Londoño, C. Yao, C. E. Costello, and A. C. Steere. 2013. A novel human autoantigen, endothelial cell growth factor, is a target of T and B cell responses in patients with Lyme disease. *Arthritis Rheum.* 65: 186–196.
65. Crowley, J. T., E. E. Drouin, A. Pianta, K. Strle, Q. Wang, C. E. Costello, and A. C. Steere. 2015. A highly expressed human protein, apolipoprotein B-100, serves as an autoantigen in a subgroup of patients with Lyme disease. *J. Infect. Dis.* 212: 1841–1850.
66. Pianta, A., S. L. Arvikar, K. Strle, E. E. Drouin, Q. Wang, C. E. Costello, and A. C. Steere. 2017. Two rheumatoid arthritis-specific autoantigens correlate microbial immunity with autoimmune responses in joints. *J. Clin. Invest.* 127: 2946–2956.
67. Tough, D. F., P. Borrow, and J. Sprent. 1996. Induction of bystander T cell proliferation by viruses and type I interferon in vivo. *Science* 272: 1947–1950.
68. Tough, D. F., X. Zhang, and J. Sprent. 2001. An IFN-γ-dependent pathway controls stimulation of memory phenotype CD8$^+$ T cell turnover in vivo by IL-12, IL-18, and IFN-γ. *J. Immunol.* 166: 6007–6011.
69. Zhang, X., S. Sun, I. Hwang, D. F. Tough, and J. Sprent. 1998. Potent and selective stimulation of memory-phenotype CD8$^+$ T cells in vivo by IL-15. *Immunity* 8: 591–599.
70. Slichter, C. K., A. McDavid, H. W. Miller, G. Finak, B. J. Seymour, J. P. McNevin, G. Diaz, J. L. Czartoski, M. J. McElrath, R. Gottardo, and M. Prlic. 2016. Distinct activation thresholds of human conventional and innate-like memory T cells. *JCI Insight* 1: 193–201.
71. McSorley, S. J. 2014. The role of non-cognate T cell stimulation during intracellular bacterial infection. *Front. Immunol.* 5: 319.
72. O'Donnell, H., and S. J. McSorley. 2014. *Salmonella* as a model for non-cognate Th1 cell stimulation. *Front. Immunol.* 5: 621.
73. Brown, C. R., and S. L. Reiner. 1998. Clearance of *Borrelia burgdorferi* may not be required for resistance to experimental lyme arthritis. *Infect. Immun.* 66: 2065–2071.
74. Ma, Y., K. P. Seiler, E. J. Eichwald, J. H. Weis, C. Teuscher, and J. J. Weis. 1998. Distinct characteristics of resistance to *Borrelia burgdorferi*-induced arthritis in C57BL/6N mice. *Infect. Immun.* 66: 161–168.
75. Cottalorda, A., C. Verschelde, A. Marçais, M. Tomkowiak, P. Musette, S. Uematsu, S. Akira, J. Marvel, and N. Bonnefoy-Berard. 2006. TLR2 engagement on CD8 T cells lowers the threshold for optimal antigen-induced T cell activation. *Eur. J. Immunol.* 36: 1684–1693.
76. Dolganiuc, A., C. Garcia, K. Kodys, and G. Szabo. 2006. Distinct Toll-like receptor expression in monocytes and T cells in chronic HCV infection. *World J. Gastroenterol.* 12: 1198–1204.